AFRL-RZ-WP-TR-2011-2005

SOFTWARE PACKAGE ON INTEGRATED NONLINEAR DYNAMIC MODELING AND FIELD ORIENTED CONTROL (FOC) OF PERMANENT MAGNET (PM) MOTOR FOR HIGH PERFORMANCE ELECTROMECHANICAL ACTUATORS (EMAs)

Quinn Leland

Mechanical Energy Conversion Branch
Power Division

Thomas X. Wu, Louis Chow, David Woodburn, Lei Zhou, Jared Bindl, Yang Hu, and Wendell Brokaw

University of Central Florida

JANUARY 2011
Interim Report

AIR FORCE RESEARCH LABORATORY
PROPULSION DIRECTORATE
WRIGHT-PATTERSON AIR FORCE BASE, OH 45433-7251
AIR FORCE MATERIEL COMMAND
UNITED STATES AIR FORCE

NOTICE AND SIGNATURE PAGE

AFRL-RZ-WP-TR-2011-2005 HAS BEEN REVIEWED AND IS APPROVED FOR PUBLICATION IN ACCORDANCE WITH THE ASSIGNED DISTRIBUTION STATEMENT.

*//signature//	//signature//
QUINN LELAND Engineer Mechanical Energy Conversion Branch	JACK VONDRELL Chief Mechanical Energy Conversion Branch

*Disseminated copies will show "//signature//" stamped or typed above the signature blocks.

REPORT DOCUMENTATION PAGE

Form Approved
OMB No. 0704-0188

1. REPORT DATE *(DD-MM-YY)*	2. REPORT TYPE	3. DATES COVERED *(From - To)*
January 2011	Interim	22 January 2008 – 04 June 2010

4. TITLE AND SUBTITLE

SOFTWARE PACKAGE ON INTEGRATED NONLINEAR DYNAMIC MODELING AND FIELD ORIENTED CONTROL (FOC) OF PERMANENT MAGNET (PM) MOTOR FOR HIGH PERFORMANCE ELECTROMECHANICAL ACTUATORS (EMAs)

5a. CONTRACT NUMBER
FA8650-09-2-2940

5b. GRANT NUMBER

5c. PROGRAM ELEMENT NUMBER
0602203F

6. AUTHOR(S)

Quinn Leland (Power Division, Mechanical Energy Conversion Branch (AFRL/RZPG)
Thomas X. Wu, Louis Chow, David Woodburn, Lei Zhou Jared Bindl, Yang Hu, and Wendell Brokaw (University of Central Florida)

5d. PROJECT NUMBER
3145

5e. TASK NUMBER
20

5f. WORK UNIT NUMBER
314520CB

7. PERFORMING ORGANIZATION NAME(S) AND ADDRESS(ES)

(Power Division, Mechanical Energy Conversion Branch (AFRL/RZPG)
Air Force Research Laboratory, Propulsion Directorate
Wright-Patterson Air Force Base, OH 45433-7251
Air Force Materiel Command
United States Air Force

University of Central Florida
4000 Central Florida Blvd.
Orlando, FL 32816

University of Dayton
444 E. 2nd St.
Dayton, OH 45402

8. PERFORMING ORGANIZATION REPORT NUMBER

9. SPONSORING/MONITORING AGENCY NAME(S) AND ADDRESS(ES)

Air Force Research Laboratory
Propulsion Directorate
Wright-Patterson Air Force Base, OH 45433-7251
Air Force Materiel Command
United States Air Force

10. SPONSORING/MONITORING AGENCY ACRONYM(S)
AFRL/RZPG

11. SPONSORING/MONITORING AGENCY REPORT NUMBER(S)
AFRL-RZ-WP-TR-2011-2005

12. DISTRIBUTION/AVAILABILITY STATEMENT
Approved for public release; distribution unlimited.

13. SUPPLEMENTARY NOTES
PAO Case Number: 88ABW-2010-6498; Clearance Date: 13 December 2010. Report contains color.

14. ABSTRACT

The development of all-electric aircraft is a high priority in the avionics community. Current aircraft use a combination of hydraulic, pneumatic, and electric systems for flight control. However, the expectation for future airplanes is a single, electric system using electromechanical actuators (EMAs). Such a system would reduce the cost to build, operate, and maintain aircraft. It would also make aircraft lighter, more reliable, safer, and more easily reconfigurable, reducing the turnaround for new technology. One of the greatest hurdles to replacing all hydraulic actuators with EMAs is heat generation, a consequence of the absence of cooling hydraulic fluid. Accurately quantifying the heat generated is complicated by the highly transient and localized nature of the power demands of an EMA's motor, an especially significant issue in aircraft. Thus, accurate modeling must be dynamic.

15. SUBJECT TERMS

integrated, nonlinear, dynamic, field oriented control, permanent magnet, EMA, electromechanical actuator, lumped-element model, inductance, flux linkage, all-electric aircraft, coenergy, eddy current, three phase, convergence, direct-quadrature reference frame

16. SECURITY CLASSIFICATION OF:			17. LIMITATION OF ABSTRACT:	18. NUMBER OF PAGES	19a. NAME OF RESPONSIBLE PERSON (Monitor)
a. REPORT	b. ABSTRACT	c. THIS PAGE			Quinn Leland
Unclassified	Unclassified	Unclassified	SAR	54	19b. TELEPHONE NUMBER *(Include Area Code)* N/A

Table of Contents

Part I - Technical Manual

I.) Introduction

The development of all-electric aircraft is a high priority in the avionics community. Current aircraft use a combination of hydraulic, pneumatic, and electric systems for flight control. However, the expectation for future airplanes is a single, electric system using electromechanical actuators (EMAs). Such a system would reduce the cost to build, operate, and maintain aircraft. It would also make aircraft lighter, more reliable, safer, and more easily reconfigurable, reducing the turnaround for new technology.

One of the greatest hurdles to replacing all hydraulic actuators with EMAs is heat generation, a consequence of the absence of cooling hydraulic fluid. Accurately quantifying the heat generated is complicated by the highly transient and localized nature of the power demands of an EMA's motor, an especially significant issue in aircraft. Thus, accurate modeling must be dynamic.

The parameters that characterize the motor are nonlinear functions. In steady-state analysis, these nonlinearities can simply be averaged out, and often the parameters are considered to be constant [1]. But during transient analysis these nonlinearities can become critical [2]. Consequently, time-averaged, linear models [3] are inadequate for thermal analysis and management designs. So, proper treatment of the problem requires dynamic, nonlinear analysis.

The motor parameters can be determined by careful experimentation [2-3], but this is a time intensive process and can be expensive especially when considering multiple potential designs for a motor. Jens Otto suggested using a reduced order coenergy model [4], which yielded results comparable to FEM results. Likewise, Roshen considered more involved empirical formulas which accounted for excess eddy current losses [5].

Through FEM modeling, the nonlinear parameters, such as self and mutual inductances of the three phase windings, can be determined [6-7]. Though dynamic FEM can be very accurate [4], such detailed simulation is very slow. Fortunately, FEM is only necessary to quantify the parameters; it is not necessary for simulating the motor over lengthy mission profiles. Instead, a nonlinear, lumped element model (NL-LEM) can use the parameters from the FEM model and then dynamically simulate the motor just as accurately as the FEM model but at a much lower computational cost. To our knowledge, we are the first to address the nonlinear dynamic modeling of a permanent magnet motor and describe both the control and thermal performance of the motor in following highly transient mission profiles.

Figure 1.1 is the 3-D model of a typical Permanent Magnet Synchronous Machine (PMSM) servo motor. This design features a 12-slot stator and a 10-pole rotor (Figure 1.2). In the following, we will discuss the procedures for electrical and thermal modeling.

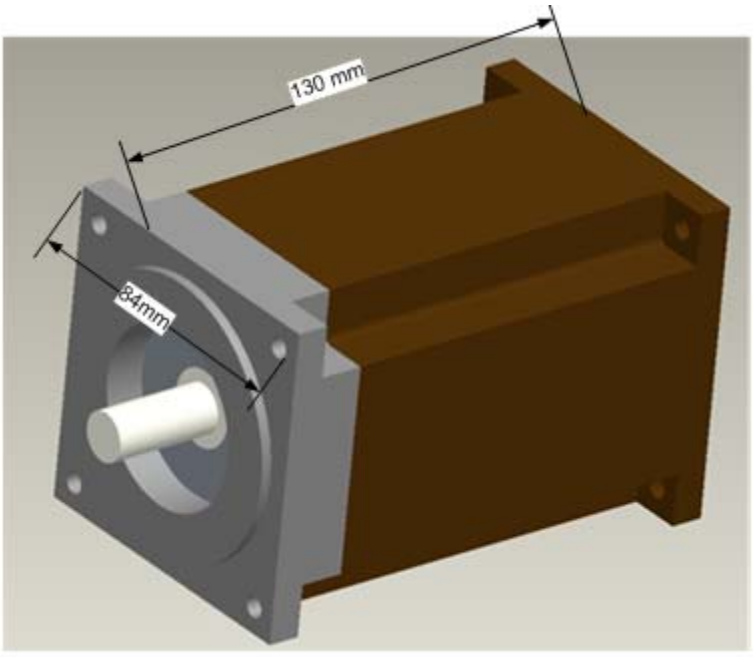

Figure 1.1. 3-D model of the PMSM motor design.

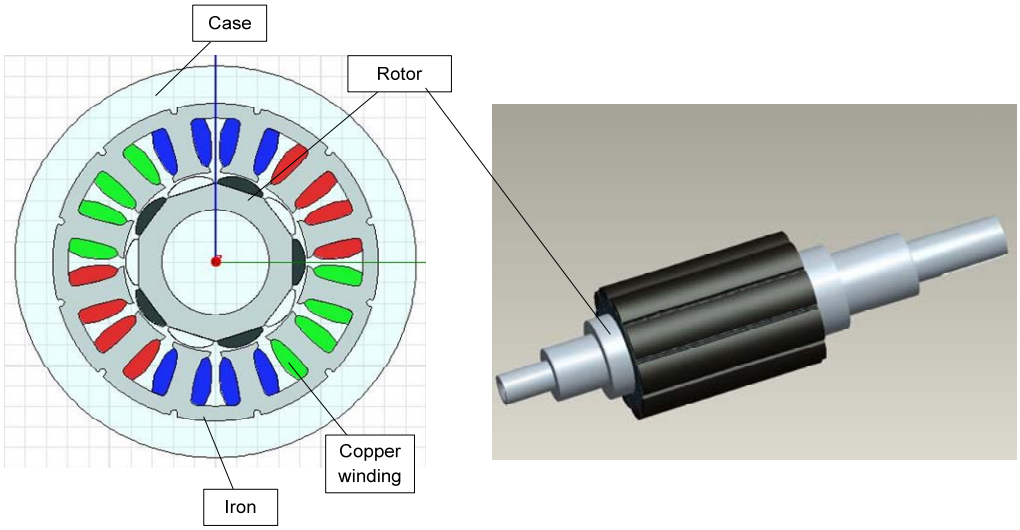

Figure 1.2. Cross-section of motor and rotor.

II.) Simulation Flow Chart

Before describing the details of the simulation, we give the overall flow chart in Figure 1.3 as follows:

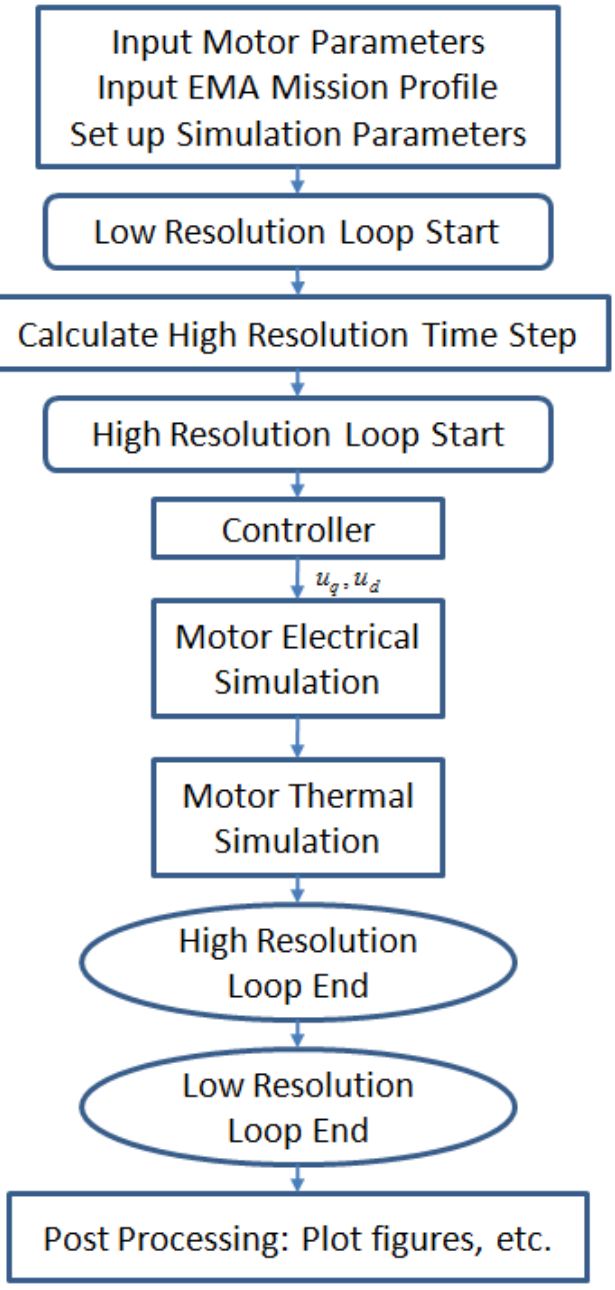

Figure 1.3: Flow chart for simulation

For the motor electrical simulation block, the flow chart is given in Figure 1.4.

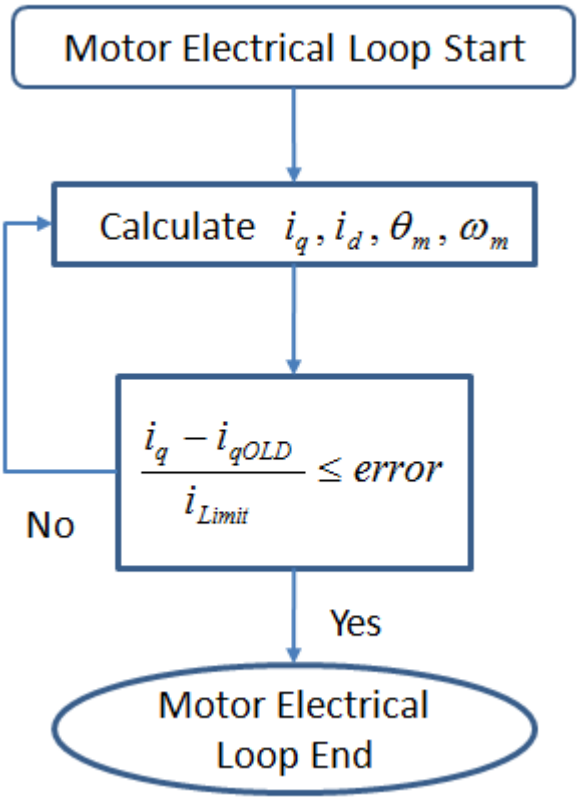

Figure 1.4: Flow chart for motor electrical simulation

III.) Electrical Model

1. Dynamical Equations

The motor dynamics are modeled by four primary dynamical equations in direct-quadrature reference frame (dq0):

$$u_d = R_s i_d + L_d \frac{di_d}{dt} - \omega_{me} L_q i_q \quad (1)$$

$$u_q = R_s i_q + L_q \frac{di_q}{dt} + \omega_{me} L_d i_d + \omega_{me} \lambda_{PM} \tag{2}$$

$$\tau_M = i_q \left\{ \frac{3}{4} p \cdot \left[\lambda_{PM} + i_d \cdot \left(L_d - L_q \right) \right] \right\} \tag{3}$$

$$\tau_M = \tau_L + \frac{2}{p} \left(I \alpha_{me} + c \omega_{me} \right) \tag{4}$$

where u_d is direct input voltage, u_q is quadrature input voltage, i_d is direct current, i_q is quadrature current, R_s is phase resistance, L_d is direct inductance, L_q is quadrature inductance, p is the number of poles, ω_{me} is the mechanical frequency multiplied by the number of pole pairs $p/2$, λ_{PM} is the flux linkage from the permanent magnet, τ_M is the motor torque generated by the magnetic fields, τ_L is the load torque, α_{me} is the mechanical angular acceleration multiplied by the number of pole pairs $p/2$, I is the rotor's moment of inertia, and c is the rotor's coefficient of friction from windage and bearings.

where u is input voltage, i_d is direct current, i_q is quadrature current, R_s is phase resistance, L_d is direct inductance, L_q is quadrature inductance, p is the number of poles, ω_{me} is the mechanical frequency multiplied by the number of pole pairs $p/2$, λ_{PM} is the flux linkage from the permanent magnet, τ_M is the motor torque generated by the magnetic fields, τ_L is the load torque, α_{me} is the mechanical angular acceleration multiplied by the number of pole pairs $p/2$, I is the rotor's moment of inertia, and c is the rotor's coefficient of friction from windage and bearings.

The motor losses are related to the motor parameters, such as R_s, c, L_d, and L_q. Since losses have an effect on motor behavior, they should be modeled through the motor parameters, not calculated in post-processing, as is often done [5]. The copper loss can be calculated as

$$P_{cu} = \left(i_a^{\,2} + i_b^{\,2} + i_c^{\,2} \right) R_s , \tag{5}$$

or equivalently

$$P_{cu} = \frac{3}{2} \left(i_d^{\,2} + i_q^{\,2} \right) R_s , \tag{6}$$

for balanced 3-phases. In either case, note that the resistance is the parameter directly associated with the power loss in the windings. Likewise, windage and bearing losses are directly associated with the coefficient of friction, c. All iron losses (hysteresis, classical eddy, and excess eddy losses) can be associated with the nonlinear inductance, L.

Much of the motor modeling research done in the past [1] and [8] and even recent work [9] use constant parameter values in simulations, although some did use nonlinear inductances [2] and [7], and [10]. Since the BH curve is nonlinear and H is a function of current, inductance is also a nonlinear function of current. For our model, we used FEM to obtain L_d and L_q as functions of i_q. At this point we are neglecting changes in i_d since our control algorithm already seeks to maintain a zero value for i_d. The inductance curves we do have were calculated in ANSYS using the magnetization curve for our particular soft-magnetic material and the geometry of our motor. The analysis was done for zero direct current and for a wide range of quadrature currents (Figure 1.5).

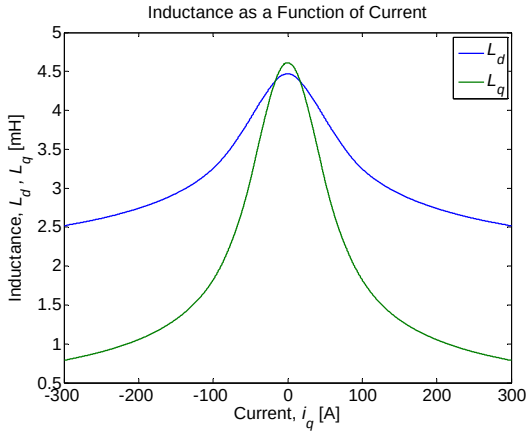

Figure. 1.5. Direct and quadrature inductance as a function of current.

2. Time Stepping

The size of variable arrays affects the speed of a simulation. Using prerecorded input profiles, high resolution is necessary to accurately capture transient moments. A uniform, high resolution would result in a very large profile. To keep our array sizes small but maintain high resolution where needed, we used a line simplification algorithm to reduce the number of points where little activity would occur. This compression technique allowed us to reduce the profiles to less than 4% of their original size.

That said, the electrical time constant is often much smaller than the time-step size of the compressed profiles. Since the frequency of the electrical component of the simulation is directly related to the first derivative of the input angular position profile for the motor, we can dynamically scale the electrical time step non-uniformly. Therefore, we had two loops, one macro loop that stepped through the elements of the profile and a nested micro loop with very small, but variable time steps for the electrical equations. The result of this apparent complication was a many-fold speed improvement. This is a tremendous advantage of not relying on MATLAB built-in ODE solvers, which do not have the advantage of knowing how big of a time step to take but must rather continually search for it.

3. Field Oriented Control (FOC)

A thorough analysis of motor heat generation should include how the motor is driven. Our control equations are derived from the primary simulation equations (1) through (4). Starting with equation (4) and noting that in (3) i_q can be factored out, we get

$$i_q \frac{\tau_M}{i_q} = \tau_L + \frac{2}{p}\left(I\alpha_{me} + c\omega_{me}\right), \tag{7}$$

which can be rearranged to be

$$i_q = \frac{\tau_L + \frac{2}{p}\left(I\alpha_{me} + c\omega_{me}\right)}{\frac{\tau_M}{i_q}}. \tag{8}$$

At this point we reinterpret α_{me} which is $d\omega_{me}/dt$ to be $e_{\omega_{me}}/dt$, where $e_{\omega_{me}}$ is the error in ω_{me}, with a tuning coefficient, k_p, in front. This gives

$$i_q{}^* = \frac{\tau_L + \frac{2}{p}\left(Ik_p \frac{e_{\omega_{me}}}{dt} + c\omega_{me}{}^*\right)}{\frac{\tau_M}{i_q}}, \tag{9}$$

where $i_q{}^*$ is the desired current for the next time step and $\omega_{me}{}^*$ is the desired next-step angular speed equal to $\omega_{me} + k_p e_{\omega_{me}}$. Using (4) to substitute for τ_L in (9), we arrive at (10):

$$i_q^* = \frac{\left(\tau_M - \frac{2}{p} I\alpha_{me} - \frac{2}{p} c\omega_{me}\right)}{\frac{\tau_M}{i_q}} + \frac{\frac{2}{p}\left(Ik_p \frac{e_{\omega_{me}}}{\Delta t} + c\omega_{me}^*\right)}{\frac{\tau_M}{i_q}} \quad . \tag{10}$$

Recalling that $\left(\omega_{me}^* - \omega_{me}\right)$ equals $k_p e_{\omega_{me}}$, (10) simplifies to

$$i_q^* = i_q + \frac{2}{p\frac{\tau_M}{i_q}}\left[I\left(k_p \frac{e_{\omega_{me}}}{\Delta t} - \alpha_{me}\right) + c\left(k_p e_{\omega_{me}}\right)\right], \tag{11}$$

This will track the desired motor velocity well, but there will be some rotor angle drift over time. To counter this drift error, we added a theta error term, $k_i e_{\theta_{me}} / dt$:

$$i_q^* = i_q + \left(k_i \frac{e_{\theta_{me}}}{dt}\right) + \frac{2}{p\frac{\tau_M}{i_q}}\left[I\left(k_p \frac{e_{\omega_{me}}}{dt} - \alpha_{me}\right) + c\left(k_p e_{\theta_{me}}\right)\right] \tag{12}$$

The k_p and k_i coefficients are the only PI values that need to be tuned in the control algorithm. For maximum efficiency, it is generally desired that the direct current be zero since any flux generated in the direct axis would not contribute to torque. However, direct current does not necessarily directly translate to direct flux. As the following equation shows, direct current can contribute to useful torque if the direct and quadrature inductances are not equal, as given in (3).

Most of the time, however, the desired direct current set point, i_d^*, should be zero. With the desired currents determined, the desired voltages can be found:

$$u_d^* = R_s i_d^* + L_d^* \frac{di_d^*}{dt} - \omega_{me}^* L_q^* i_q^* \tag{13}$$

$$u_q^* = R_s i_q^* + L_q^* \frac{di_q^*}{dt} + \omega_{me}^* L_d^* i_d^* + \omega_{me}^* \lambda_{PM}\,, \tag{14}$$

where L_d^* and L_q^* are based on the desired current values. It should be noted that while many of the variables are updated based upon the desired currents, τ_M was not updated for the control equations. This is a reasonable simplification since for a round rotor λ_{PM} is independent of θ_{me}, i_d should normally be zero, and the i_q factor is divided out:

$$\frac{\tau_M}{i_q} = \frac{3}{4} p \cdot \left[\lambda_{PM} + i_d \cdot \left(L_d - L_q\right)\right] \tag{15}$$

For the non-round rotor case, our direct interpolation method could be used to include the dependence on theta.

Even after the desired control values were calculated, the reality of limits (current and voltage) needed to be included. Instead of directly capping those values, we realized that the system converged more quickly and ran more smoothly if the functions used were all smooth [11]. For our case, we used a segmented curve of first and second-order polynomials.

IV.) Thermal Model

1. Model Setup

A lumped node thermal network is to represent the temperature of every solid part of the EMA. The thermal resistances and capacitances between the nodes can be treated as electrical resistances and capacitances. Hence the temperature of every node can be solved as the voltage in this equivalent network (Table 1.1). This approach is well developed in motor design industry [12, 13]. Some commercial motor design software package has already included the thermal network simulation, i.e. Motor-CAD [14]. Some studies have been made with FEA analysis and experimental testing have shown that such an approach is valid [15].

Table 1.1 The analogy of equivalent thermal circuit

Electrical Circuit			Thermal Circuit		
V	$[V]$	Voltage	T	$[^oC]$	Temperature
I	$[A]$	Current Flow	Q	$[W]$	Heat Flow
σ	$[1/\Omega m]$	Electrical Conductivity	κ	$[W/^oCm]$	Thermal Conductivity
R	$[\Omega]$	Resistance	R^θ	$[^oC/W]$	Thermal Resistance
C	$[F]$	Capacitance	C^θ	$[J/^oC]$	Thermal Capacitance

$$R^{\theta}_{conductive} = \frac{\Delta X}{k * A_{contact}}$$
$$R^{\theta}_{convective} = \frac{1}{h * A_{surface}} \quad (16)$$

$$C^{\theta} = \rho * V * C_p \quad (17)$$

Equations (16) and (17) show how to calculate of the R and C values for simple one-dimensional geometry. Accurate estimates for R and C values are not possible for complicated geometries such as an electric motor. The traditional lumped node thermal network is based on a "forward" direction modeling process. In this process, with all the material, geometry and construction information provided, the thermal resistance Rθ and capacitance Cθ are calculated based on empirical and theoretical relations. For example, when the winding wire type, winding structure, potting material, slot width and teeth thickness are given, the thermal resistance from winding to stator and from winding to rotor can be calculated. Because this type of approach requires large number of empirical relations to achieve high accuracy, a "reverse" modeling process is introduced in this paper. A detailed 3-D solid model of a target motor is constructed and imported to an FEA software like ANSYS [16] to perform steady-state and transient simulation. With these results we can estimate and select the values for the thermal resistances and capacitances. The advantage of this method is that we can evaluate the fidelity of the lumped node model with a real motor, add or reduce nodes to increase the model accuracy and efficiency, and estimate the maximum error between the node temperature and maximum temperature in real motor.

This procedure can also be extended to model the gear-box, motor-driver and drive-train, and even include the aircraft wing surfaces and frames. The thermal network can also be incorporated into a multi-physics model to simulate the electrical, thermal and mechanical performance of the whole EMA and its supporting structure. Once the proper thermal resistances and capacitances are selected, this simulation engine can be used with various time dependent boundary conditions during the whole mission duration, including the air temperature, aircraft speed, altitude and sunlight.

The computational requirement of such a simulation is negligible compared to the FEA simulation.

Due to the symmetry, the geometry of the model shown in Figure 1.1 is divided into a quarter section and imported into ANSYS for the FEA simulation. The nodes are numbered in Figure 1.6. These numbers are also the same as those in the lumped node network shown in Figures 1.7.

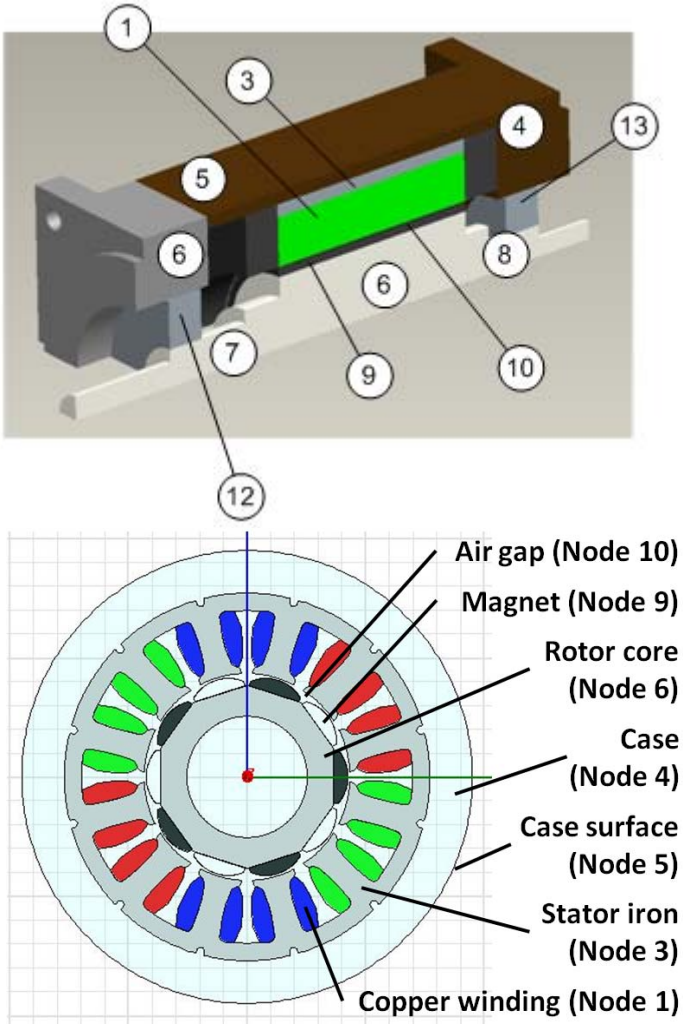

Figure 1.6. Thermal node locations on motor.

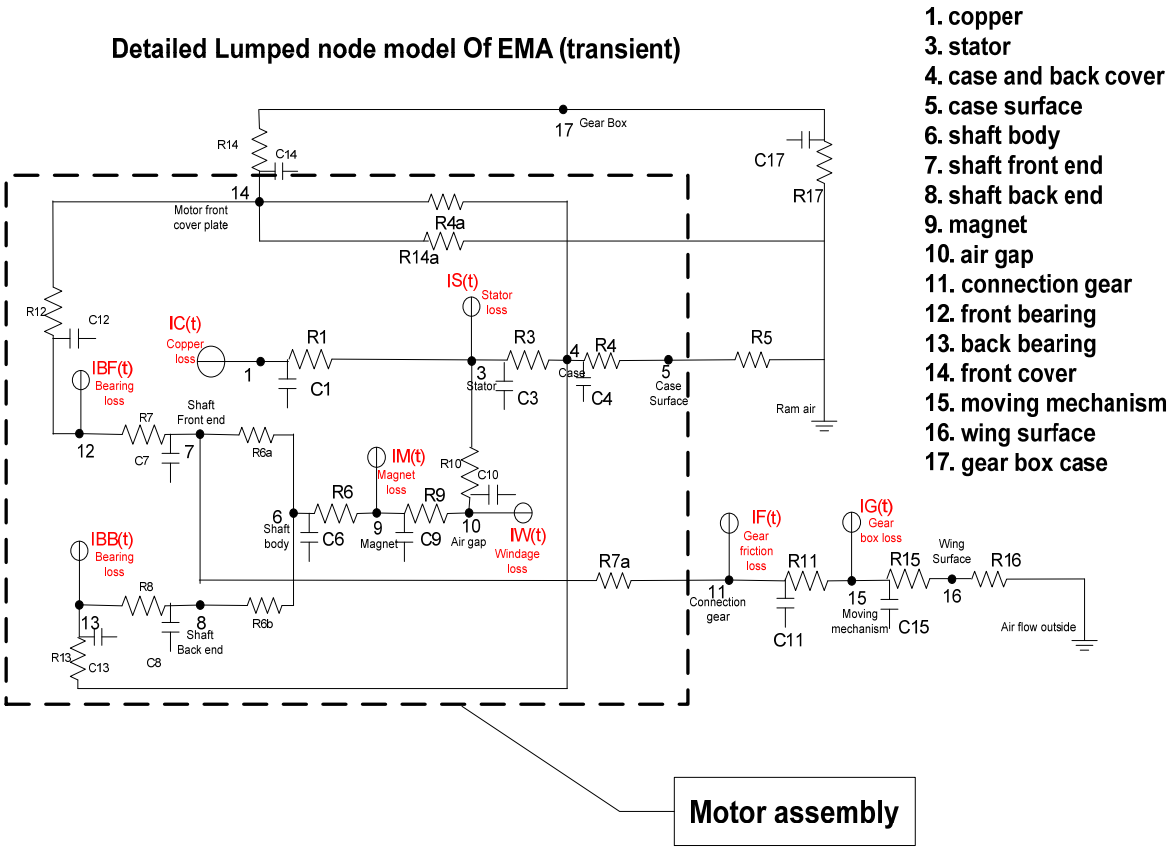

Figure 1.7. Lumped node model of EMA

2. Dynamic Thermal Equations

After all the thermal resistor and capacitor values of the lumped-node network model of the motor in Figure 5 are known, the same values of the thermal resistors and capacitors can be used to simulate the temperature response of the motor parts with any combination of heat losses and boundary conditions. For this standard resistor-capacitor electrical network, a set of first-order ordinary differential equations can be written as:

$$\frac{U_1 - U_3}{R_1} + C_1 \frac{dU_1}{dt} = I_C(t) \tag{18}$$

$$\frac{U_4 - U_3}{R_3} + \frac{U_{10} - U_3}{R_{10}} - \frac{U_1 - U_3}{R_1} + C_3 \frac{dU_3}{dt} = I_S(t) \tag{19}$$

$$(R_9 + R_{10})U_{10} = U_3 R_9 + R_{10} U_9 + R_9 R_{10} I_W(t) \tag{20}$$

$$\frac{U_6 - U_8}{R_{6b}} - \frac{U_{13} - U_8}{R_8} - C_8 \frac{dU_8}{dt} = 0 \tag{21}$$

$$\frac{U_{13} - U_4}{R_{13}} - \frac{U_{13} - U_8}{R_8} + C_{13} \frac{dU_{13}}{dt} = I_{BB}(t) \tag{22}$$

$$\frac{U_{14} - U_4}{R_{4a}} + \frac{U_{13} - U_4}{R_{13}} + \frac{U_4 - U_3}{R_3} - \frac{U_4 - U_5}{R_4} - C_4 \frac{dU_4}{dt} = 0 \tag{23}$$

$$\frac{U_{12} - U_{14}}{R_{12}} + \frac{U_7 - U_{12}}{R_7} - C_{12} \frac{dU_{12}}{dt} = I_{BF}(t) \tag{24}$$

$$\frac{U_9 - U_6}{R_6} - \frac{U_{10} - U_9}{R_9} + C_9 \frac{dU_9}{dt} = I_M(t) \tag{25}$$

$$\frac{U_6 - U_7}{R_{6a}} + \frac{U_6 - U_8}{R_{6b}} - \frac{U_9 - U_6}{R_6} + C_6 \frac{dU_6}{dt} = 0 \tag{26}$$

$$\frac{U_7 - U_{12}}{R_7} - \frac{U_6 - U_7}{R_{6a}} + C_7 \frac{dU_7}{dt} = -I_{R7a} \tag{27}$$

$$\frac{U_{12} - U_{14}}{R_{12}} - \frac{U_{14} - U_4}{R_{4a}} + C_{14} \frac{dU_{14}}{dt} = I_{R14} \tag{28}$$

Because the time constant (about 10 ms) for the thermal component is much larger than for the electrical component in our case, the thermal component was calculated less often, thereby increasing the speed of the simulation.

V.) References

1. Shi, K. L., Chan, T. F., Wong, Y. K., Ho, S. L. "Modeling and Simulation of the Three-phase Induction Motor Using Simulink," *Int. J. Elect. Enging. Educ.*, Vol. 36, pp. 163-172., Manchester U.P., Great Britain, 1999.
2. Lipo, Thomas A., Consoli, Alfio, "Modeling and Simulation of Induction Motors with Saturable Leakage Reactances," *IEEE Transactions on Industry Applications*, Vol. IA-20, No. 1, pp. 180-189, 1984.

3. Soe, Nyein N., Yee, Thet T. H., Aung, S. S., "Dynamic Modeling and Simulation of Three-phase Small Power Induction Motor," *World Academy of Science, Engineering and Technology*, Vol. 42, No. 79, pp. 421-424, 2008.
4. Otto, Jens, "Dynamic Simulation of Electromechanical Systems using ANSYS and CASPOC," *2002 International ANSYS Conference*, ANSYS, 2002.
5. Roshen, Waseem, "Iron Loss Model for PM Synchronous Motors in Transportation," *2005 IEEE Conference on Vehicle Power and Propulsion*, pp. 4, ISBN: 0-7803-9280-9, 2005.
6. Dolinar, D., Weerdt, R. De, Freeman, E. M., "Calculation of Two-axis Induction Motor Model Parameters Using Finite Elements," *IEEE Transactions on Energy Conversion*, Vol. 12, No. 2, pp. 133-142, 1997.
7. Topcu, E. E., Kamis, Z.,Yuksel, I., "Simplified numerical solution of electromechanical systems by look-up tables," *Mechatronics*, Vol. 18, No. 10, pp. 559-565, Elsevier, 2008.
8. Mohamed, M. A., Nagrial, M. H., "Modelling and Simulation of Vector-controlled Reluctance Motors Drive System," *International Conference on Simulation*, No. 457, pp. 380-384, ISBN: 0-85296-709-8, 1998.
9. Sun, Fengchun, Li, Jian, Sun, Liqing, Zhai, Li, Cguo, Fen, "Modeling and Simulation of Vector Control AC Motor Used by Electric Vehicle," *Journal of Asian Electric Vehicles*, Vol. 3, No. 1, pp. 669-672, Asian Electric Vehicle Society, 2005.
10. Demerdash, N. A., Gillott, D. H., "A New Approach for Determination of Eddy Current and Flux Penetration in Nonlinear Ferromagnetic Materials," *IEEE Trans. MAG-10*, pp. 682-685, 1974.
11. Merzouki, R., Cadiou, J. C., "Estimation of backlash phenomenon in the electromechanical actuator," *Control Engineering Practice*, Vol. 13, No. 8, pp. 973-983, Elsevier, 2004.
12. Mellor, P.H., Roberts, D., Turner, D. R., "Lumped parameter thermal model for electrical machines of TEFC design", IEEE Proc-B, Vol 138, No5, Sept. 1991.
13. DiGerlando, A., Vistoilo, I., "Thermal network of induction motors for steady state and transient operations analysis", ICEM 1994, Paris.
14. Motor-CAD v3.1.7, Motor Design Ltd, www.motor-design.com.
15. Y.K. Chin, D.A. Staton, "Transient thermal analysis using both lumped-circuit approach and finite element method of a permanent magnet traction motor", IEEE AFRICON 2004.
16. ANSYS V12.0., ANSYS, Inc., www.ansys.com.

Part II – User's Manual

I.) Introduction

a. Purpose of the Software

This software provides integrated non-linear dynamic modeling including both electrical model and thermal model together with a field oriented control scheme. Different motor configurations can be entered into the software. The simulation provides the user with all the necessary motor information, such as: mission profile following, motor torque, motor current, phase voltage, input power, power losses in the windings, and a thermal profile. This comprehensive and detailed look at motor control together with heat generation and transfer will provide solid foundation for users to design highly efficient EMAs.

b. Software Capability

Package of a nonlinear dynamic modeling of a permanent magnet motor that describes both the control and thermal performance of the motor in following highly transient mission profiles. One of the most attractive features of this model is that it is able to incorporate various motor designs. The software manual assumes that the mission profile is provided to the user. For users familiar with control coding will be able to manipulate some constants in the control helping to tune for their specific motor designs.

c. User Privileges

The main advantages to the user is to put in their own motor parameters for alternate designs and test whether the design is capable of providing proper control and also find out the thermal performance. The motor parameter code (located in Appendix A) contains a variety of values that must be determined by the user if an alternate design is used. Values such as phase resistance, number of magnetic poles, and the moment of inertia must be determined. Motor limitations are also set in this file to ensure that these limits are not exceeded during operation. The inductance values, as well as the thermal resistance and capacitance values, can be obtained from FEM models. If a new motor model is to be used that maintains the non-linear nature of the simulation, the new inductance values, thermal resistance and capacitance, should be recalculated using FEM. Although determining these values is outside the scope of

this manual, the user is able to manipulate any of the data inside the motor simulation to suit the needs of their design.

II.) Input Parameters

There are the two file names 'motorParameter' and 'missionProfile.xlsx' for input motor parameters and mission profiles.

motorParameters.m contains motor parameters specific to a particular motor design as well as calculated parameters. If you are to change the name of this folder or make a new motor design, the new name of the folder must be input into the main program. The code is displayed in Part IV but these parameters show the motor parameters for this particular example. These values can be changed to accommodate other motor/EMA designs.

Tables 2.1-2.4 summarize the input parameters in motorParameters.m.

Table 2.1. Motor Electrical Parameters

Motor Electrical Parameters	Explanations	Units	Source
Rs_room	phase resistance at room temperature	Ω	FEM or Measurement
p	number of poles		Given
I	inertia moment of rotor	kg m^2	Given
c	friction coefficient	kg m^2/s	Given
lambdaPM	permanent magnet flux amplitude λ_{PM}	Wb	FEM or Measurement
LdSN	array of direct inductance L_d corresponding to current array i_q	H	FEM or Measurement
LqSN	array of quadrature inductance L_q corresponding to current array i_q	H	FEM or Measurement
i_q	array of quadrature current	A	Given

Table 2.2. Motor Thermal Parameters

Motor Thermal Parameters	Explanations	Units	Source
Rth	thermal resistance	$^{o}C/W$	FEM
Cth	thermal capacitance	$J/^{o}C$	FEM
Troom	room temperature	^{o}C	Given
IC	winding loss	W	Electrical Simulation
IS	stator loss	W	Electrical Simulation
IW	winding loss	W	Electrical Simulation
IBB	rear bearing loss	W	Mechanical Simulation
IBF	front bearing loss	W	Mechanical Simulation
IM	magnet loss	W	Electrical Simulation
IR7a	conduction heat loss to gear box axle	W	FEM
IR14	conduction heat loss to gear box case	W	FEM

Table 2.3. Drive Train Parameters

Drive Train Parameters	Explanations	Units	Source
Ncr	total coupling ratio	rad/m	Given
effDrive	drive train efficiency		Given
theta_meIntial	initial rotor angle multiply p/2 when stroke is 0	rad	Given

Table 2.4. Simulation Limits (These parameters are given.)

Simulation Limits	Explanations	Units
xMinLim	minimum value of stroke	m
xMaxLim	maximum value of stroke	m
tauMLim	motor torque limit	N m
uLim	voltage limit	V
iLim	current limit	A
didtLim	current change rate limit	A/s
vLim	speed limit	m/s

Excel file missionProfile.xlsx provides data for mission profile. The mission profile data is assumed to have been provided already and is not subject for discussion in this manual. The input parameters in mission profile is summarized in Table 5.

Table 2.5. Mission Profile Parameters

(may come from aerodynamic measurement or simulation)

Mission Profile Parameters	Explanations	Units
tN	array for time	s
xSN	array for stroke profile	M
FLN	array for load force profile	N

Due to the fact that there can be various mission profiles and motor designs it is important to ensure that your file names in the 'FOC' folder match the file names as represented in the code above.

There are also input parameters used to set up simulation. These parameters are summarized in Table 2.6.

Table 2.6. Simulation Parameters (These parameters are given.)

Simulation Parameters	Explanations	Units
spc	samples per cycle of highest frequency	
tauTh	thermal time constant	s
kp	proportional parameter for PI controller	
ki	integral parameter for PI controller	A s/rad
alpha_dt	forward time-stepping weight for implicit algorithm in electrical loop	
epsilon	error for electrical convergence loop	
Ncvg	maximum number of convergence iterations	

If the experience of the user is adequate in the design of the control scheme, there are few parameters that can be changed to decrease error in the ability for the motor to follow the flight profile data. Users can change the proportional constant, or k_p value, and the integral constant, or k_i value of the control.

```
38
39      % Set PI coefficients.
40 -    kp = 0.1;     % []
41 -    ki = 0.0001; % [A s/rad]
42
```

```
221
222         % Get iqS.
223 -       tauM_iq = 3*p/4*(lambdaPM + id*(Ld-Lq)); % [N m/A]
224 -       iqS = iq + 2/(p*tauM_iq)*(I*(kp*eOmega_me/dtE - alpha_me) + ...
225             c*(kp*eOmega_me)) + ki*eTheta_me/dtE; % [A]
226
227         % Set idS.
228 -       idS = 0; % id should almost always be zero [A]
229
230         % Rate limit iqS (reduces transients).
231 -       diqdtS = (iqS-iq)/dtE; % Predicted current rate [A/s]
232 -       diqdtS = sign(diqdtS)*min([didtLim,abs(diqdtS)]); % Cap diqdt [A/s]
233 -       iqS = iq + diqdtS*dtE; % Rebuilt iqS [A]
234
235         % Saturation limit abs of iqS.
236 -       iqS = sign(iqS)*((abs(iqS)<i3)*(abs(iqS) - (abs(iqS)>=i1)*...
237             ((abs(iqS)-iLim*(1-rSat))^2)/(4*iLim*rSat)) + ...
238             (abs(iqS)>=i3)*iLim); % [A]
239
240 -       omega_meP = omega_me + (kp*eOmega_me);
```

Two parameters, alpha_dt and beta_dt located in the main code are weighted averages used in calculating next step values. Generally the beta value is set to .5 but can be altered at the user's discretion for algorithm convergence. Another parameter that can be changed to help improve design is spc or samples per frequency as shown below.

```
33      % ------------------------------------------------------
34      % Set up simulation parameters.
35      % ------------------------------------------------------
36 -    spc = 10;                % Samples per cycle of highest frequency
37 -    tauTh = 0.01;            % Thermal time constant [s]
38
39      % Set PI coefficients.
40 -    kp = 0.1;     % []
41 -    ki = 0.0001; % [A s/rad]
42
43      % Set differential time-stepping weights.
44 -    alpha_dt = 0.5;
45 -    beta_dt = 1 - alpha_dt;
46
```

III.) Software Startup

1. Once all the proper m-files are verified click on the ‘Start Menu’ and open the MATLAB software through the program listing.
2. Once MATLAB is open go to ‘File’ and click on ‘Open’
3. Go to through the above mentioned directory path to find the ‘FOC’ folder
4. Click on the ‘FOC’ folder and then click on the file name ‘FOC.m’
5. The following code should be displayed in the MATLAB editor screen

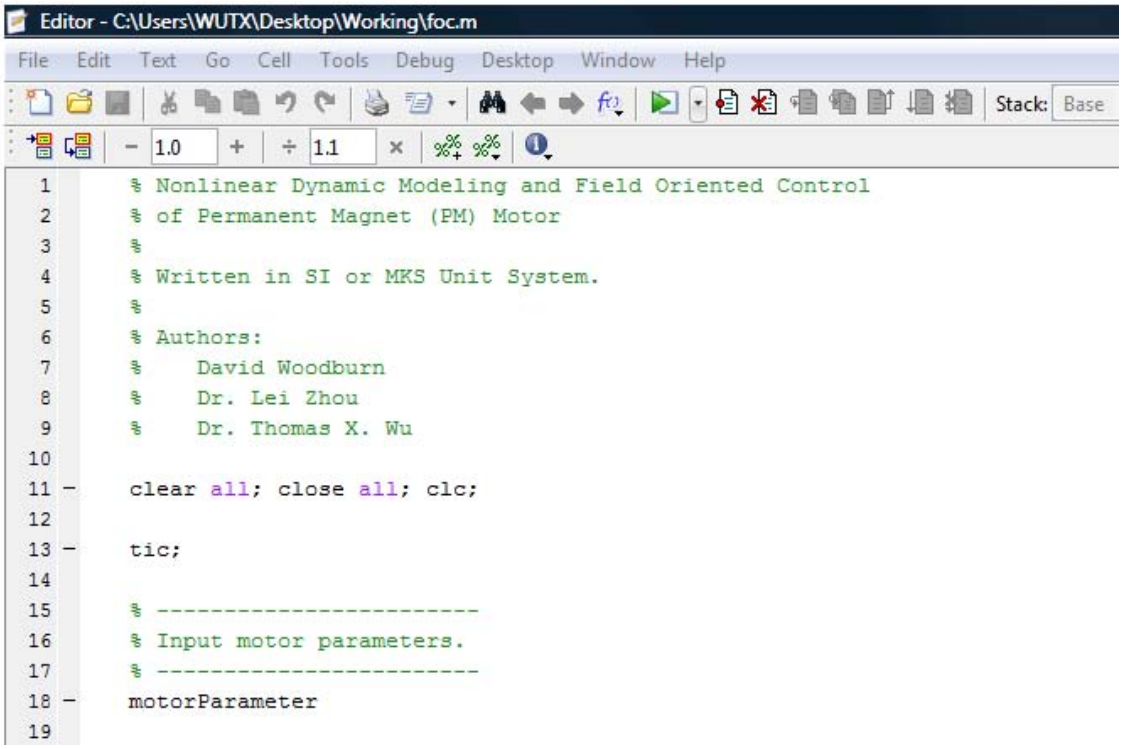

IV.) Software Execution and Procedure

1. In order to run the simulation you can either click in the editor window and press the F5 shortcut key, or click the run button at the top of the editor window.

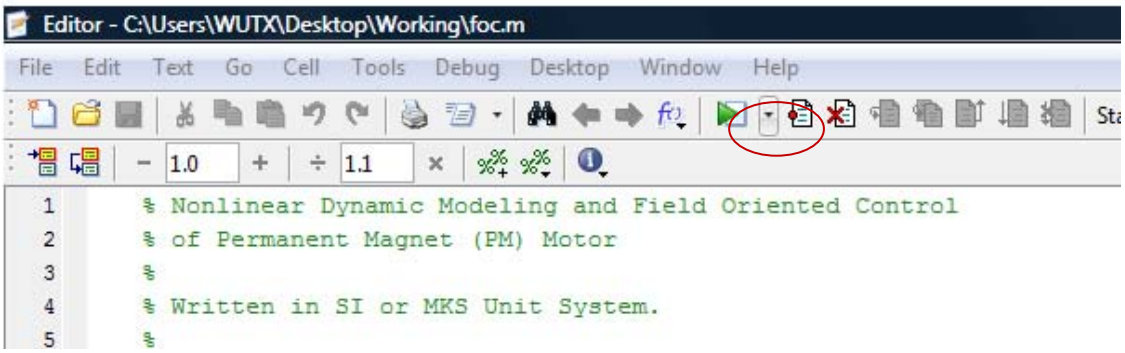

2. The following menu will pop up to add the foc.m file to the MATLAB path.

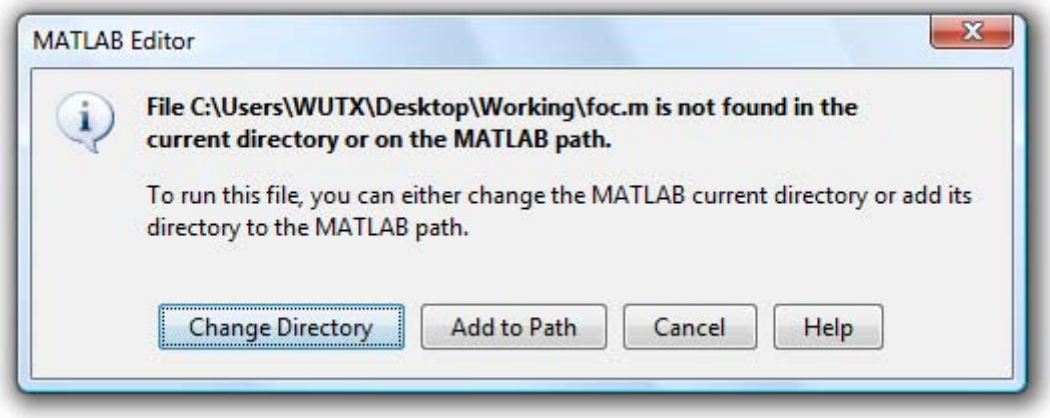

- Click Change Directory. Different versions of MATLAB will show different popup boxes when the directory is not specified. Simply ensure that all the files needed to run the program are located in the same folder before changing the path.

3. The simulation will begin running. The runtime will vary based on the system.

There will be a statistical report and a total of 9 graphs displayed as well once the simulation is finished.

V.) Output Parameters

The Output parameters are summarized in Tables 2.7 and 2.8 for reporting statistics and plot figures.

Table 2.7. Output Parameters to Report Statistics

Parameters	Explanations	Units
PcuMean	mean winding copper loss	W
tauMMax	maximum motor torque	N m
FMax	maximum actuator force	N
vMax	maximum actuator velocity	m/s
aMax	maximum acceleration	m/s^2
dtMax	maximum macro time step	s
dtEMax	maximum electrical time step	s
dtEMin	minimum electrical time step	s

Table 2.8. Output Parameters in Figures

Output Parameters	Explanations	Units
tNR	array for output time sequence	s
xN	array for actual stroke	m
tauMN	array for motor torque	N m
udN	array for direct voltage	V
uqN	array for quadrature voltage	V
idN	array for direct current	A
iqN	array for quadrature current	A
PcuN	array for instantaneous copper loss	W
PinN	array for instantaneous input power	W
TthN	2D array for temperature at different nodes	^oC

VI.) Expected Results

The simulation has fully run when the following statistics are displayed in the command window to include:

Mean winding power loss, max motor torque, max actuator force, max velocity, max acceleration, min electrical time step, max electrical time step and the total elapsed time for the program to run.

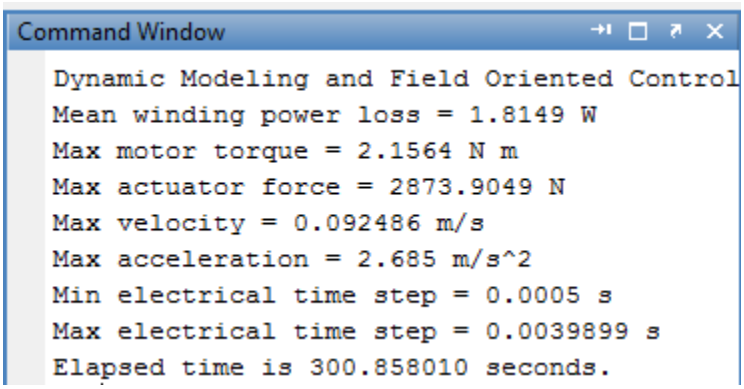

Also figures are plotted are a result of the flight mission profile used specific to this manual and will vary based on other motor parameters and flight mission data. This profile was a five minute section of a full flight profile. Acceptable values will be specific each set of parameters or profile data; however, some generalizations can be made about parameters such as power loss.

1. The stroke profile shows that movement of the shaft in the EMA. The green line represents the actual movement of the actuator based on the mission profile. The blue line is the desired movement of the EMA. It is hard to see the blue because the green is covering indicating good control. The desired stroke is in excel file missionProfile.xlsx. The actual stroke is saved in strokeActual.xlsx.

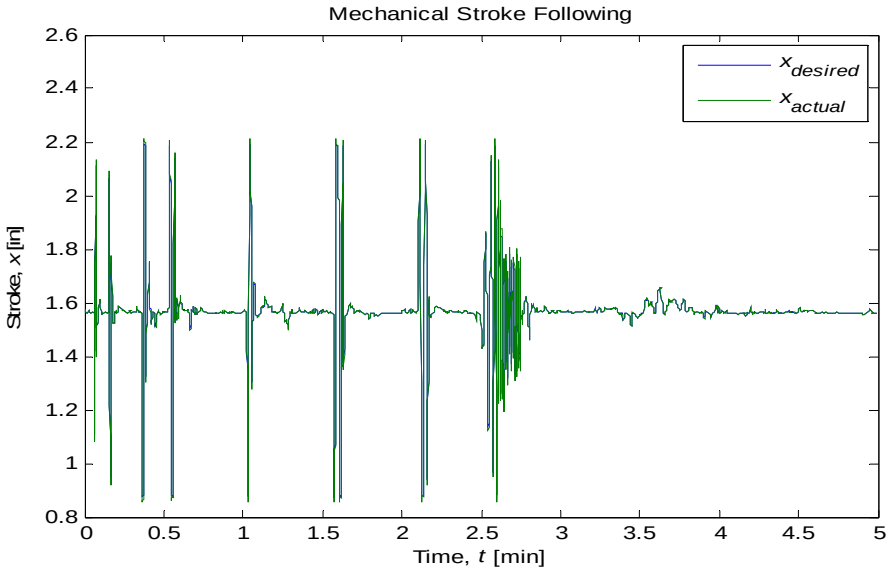

Figure 2.1 (a): EMA stroke

To further see the accuracy of the stroke following plot, a zoomed section of Figure 1 is shown below.

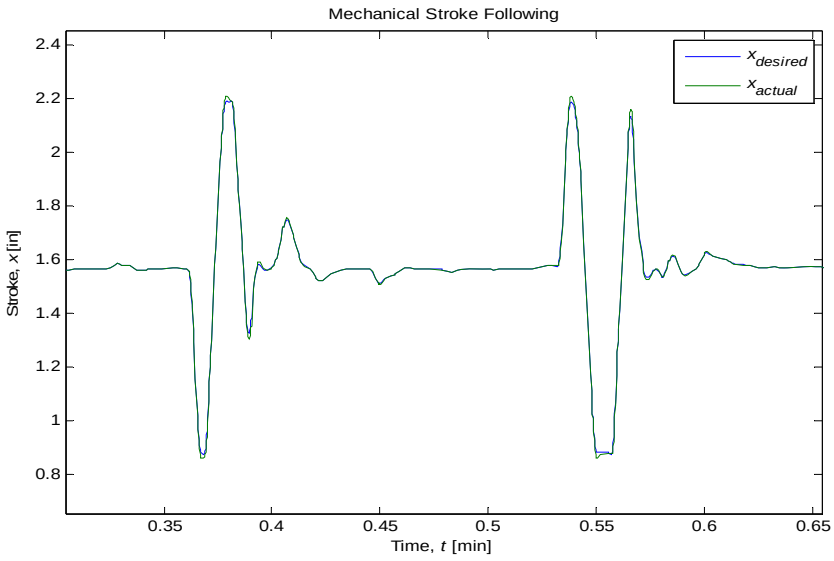

Figure 2.1 (b): Zoomed section of stroke

2. In the following Figure 2.2 (a) and (b), the load force from mission profile and load torque converted by

$$\tau_L = \frac{F_{Load}}{N_{cr}\eta_{drive}}$$

where N_{cr} is coupling ratio and η_{drive} is drive train efficiency. In Figure 2.2 (c), the magnetic torque is shown. Comparing Figure 2.2 (b) and (c), we found they are close. This is because the moment of inertia of the motor we used is small. The magnetic torque and load torque are related by:

$$J\frac{d^2\omega_m}{dt^2} = \tau_M - \tau_L$$

The magnetic torque is saved in Excel file tauM.xlsx.

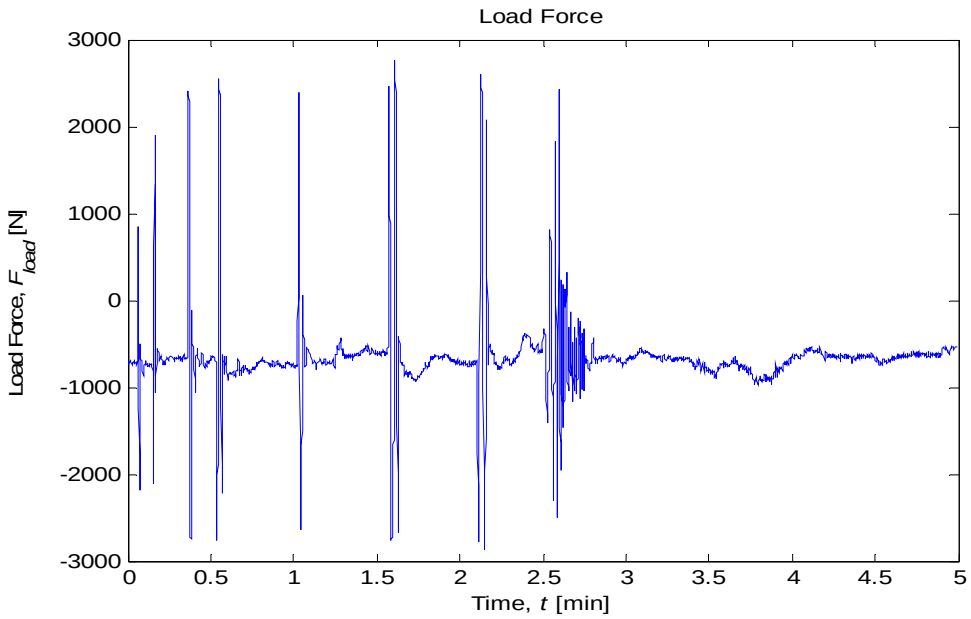

Figure 2.2(a): Load Force

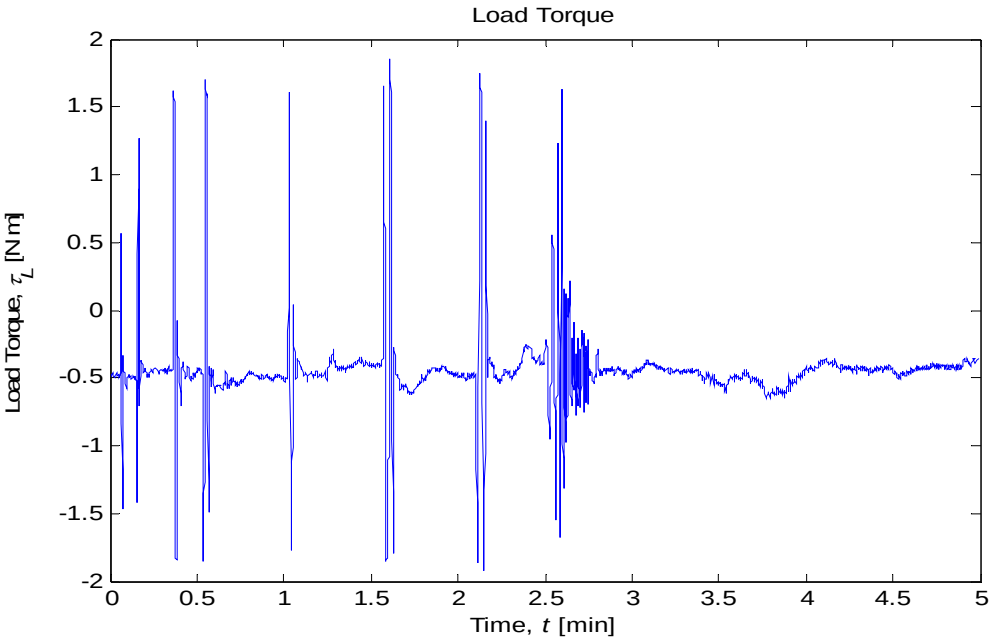

Figure 2.2(b): Load Torque

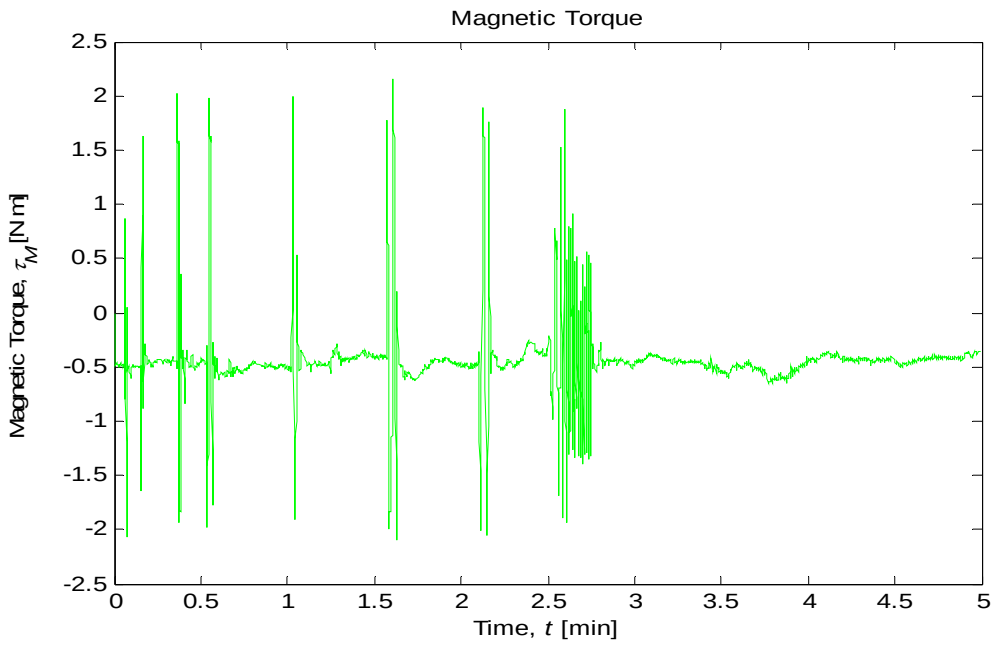

Figure 2.2(c): Magnetic Force

3. The dq currents provided to the motor are represented in Figure 2.3. Notice that the current i_d nearly constant around 0 and doesn't exceed the dotted blue line limitations. This is a proper reading as direct current does not contribute to the rotation of the rotor. Only i_q contributes to the torque as seen by the variation in the green line. The dotted green lines represent current limits of the motor. The current results are saved in Excel file idiq.xlsx.

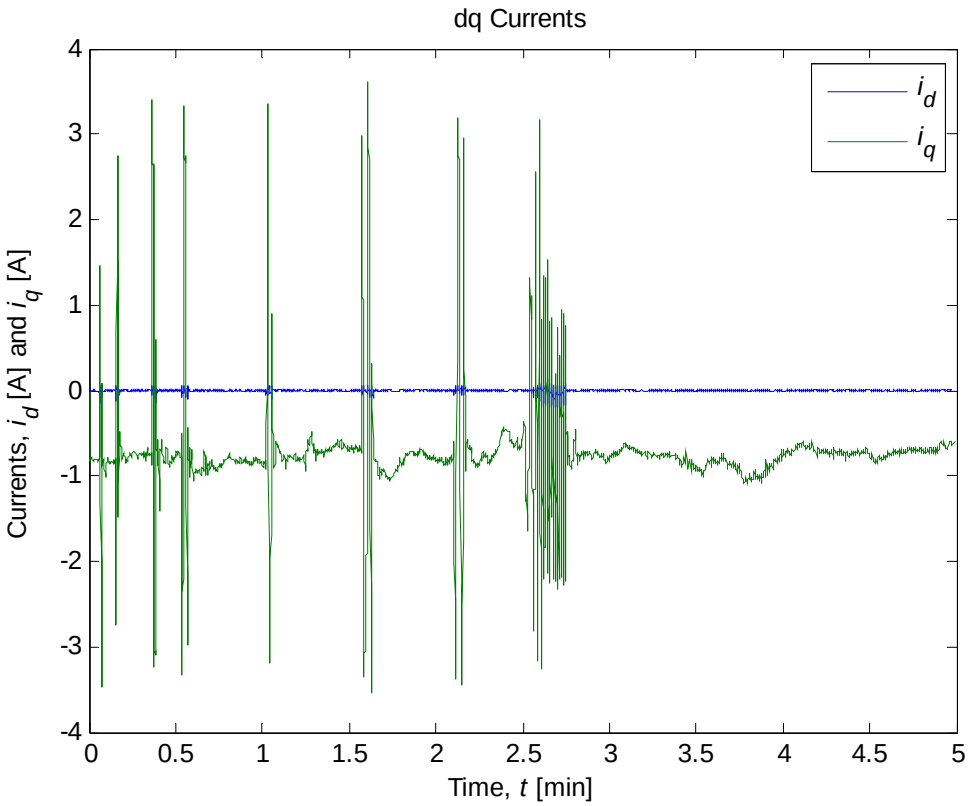

Figure 2.3: Direct and quadrature currents

4. The direct and quadrature voltages are shown here in Figure 2.4 and are similar to the currents. The direct voltage should remain around 0 and the quadrature voltage should contribute to the requirements of the selected flight profile.

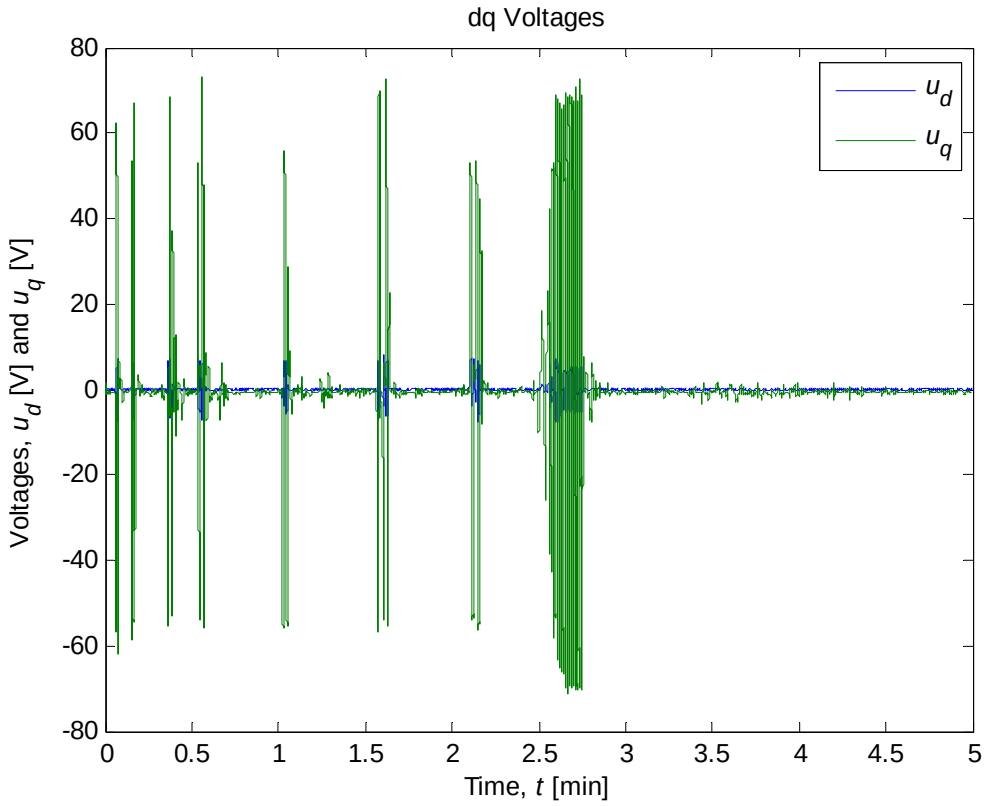

Figure 2.4 (a): Direct and quadrature voltages

The u_d voltage does not vary too much and generally stays around zero as seen in the zoomed section of the graph. The voltage results are saved in Excel file uduq.xlsx.

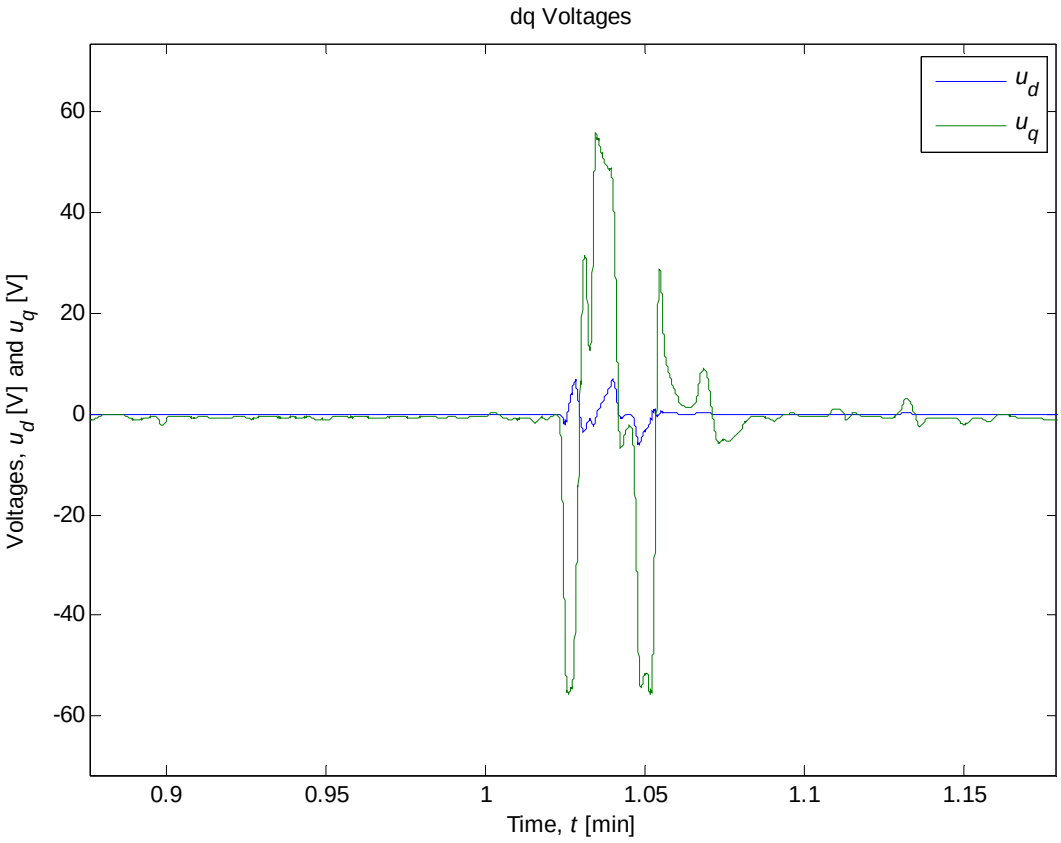

Figure 2.4 (b): Zoomed in Section of Direct and Quadrature Voltages

5. The copper winding inside the motor contain the highest source of heat. The transient heat analysis is represented here with peak values near 12 Watts which is much higher than the steady state power loss. The results are saved in Excel file Pcu.xlsx.

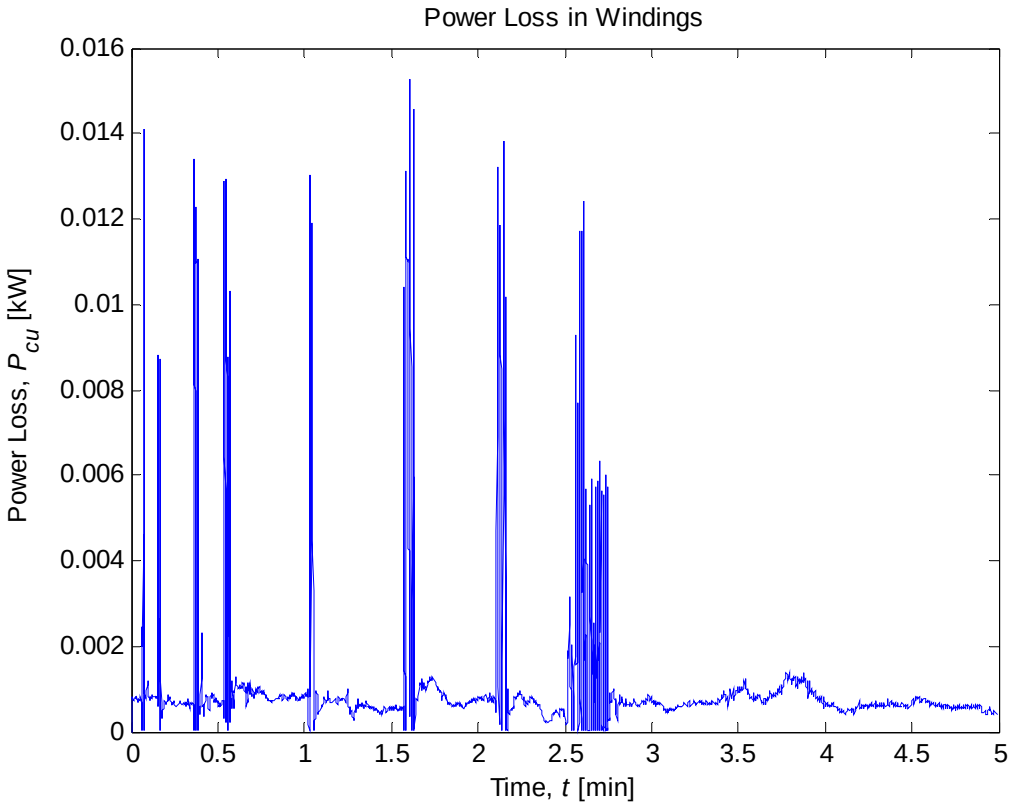

Figure 2.5: Power loss in the motor windings

6. Of great interest to power systems engineers is the power in (positive values) and out (negative values) of the motor. The power out is often called regenerative power. Here we show the power in and out of the motor in Figure 2.6. The results are saved in Excel file Pin.xlsx.

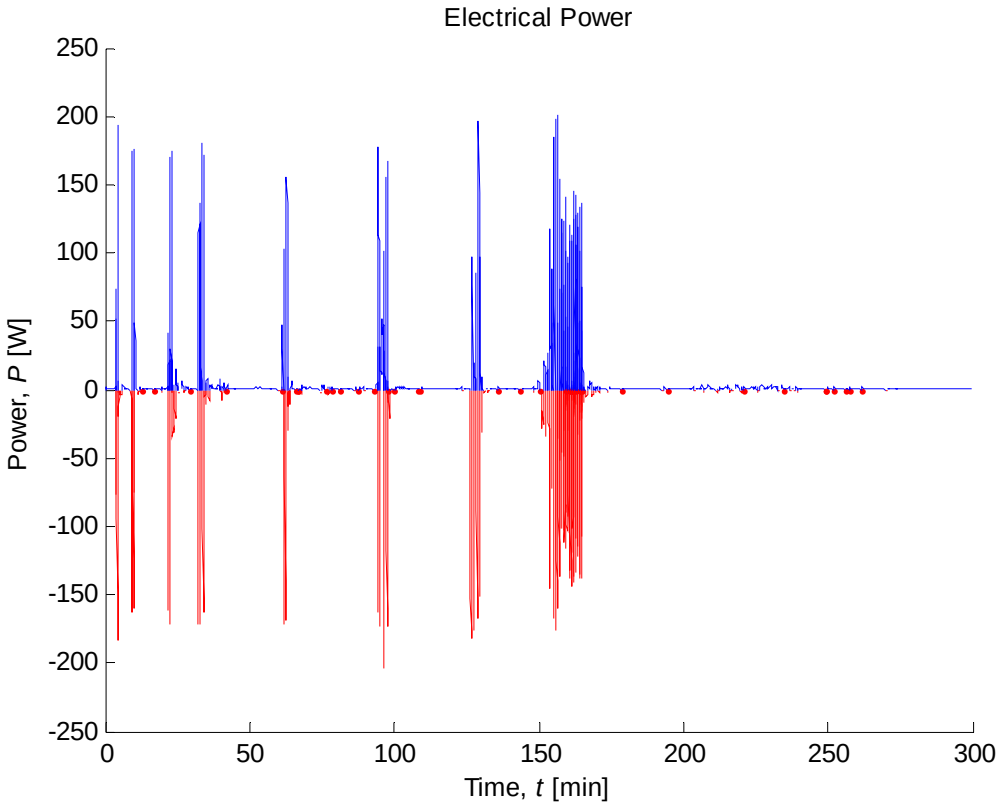

Figure 2.6: Electric input power and regenerative power

7. The temperature profiles for various nodes taken from different areas of the motor are shown below. The highest temperatures pertain to the nodes closest to the copper windings. The ambient temperature was held at 22 °C. This flight profile showed only a 0.4ºC temperature increase over 5 minute period. The results are saved in temperature.xlsx.

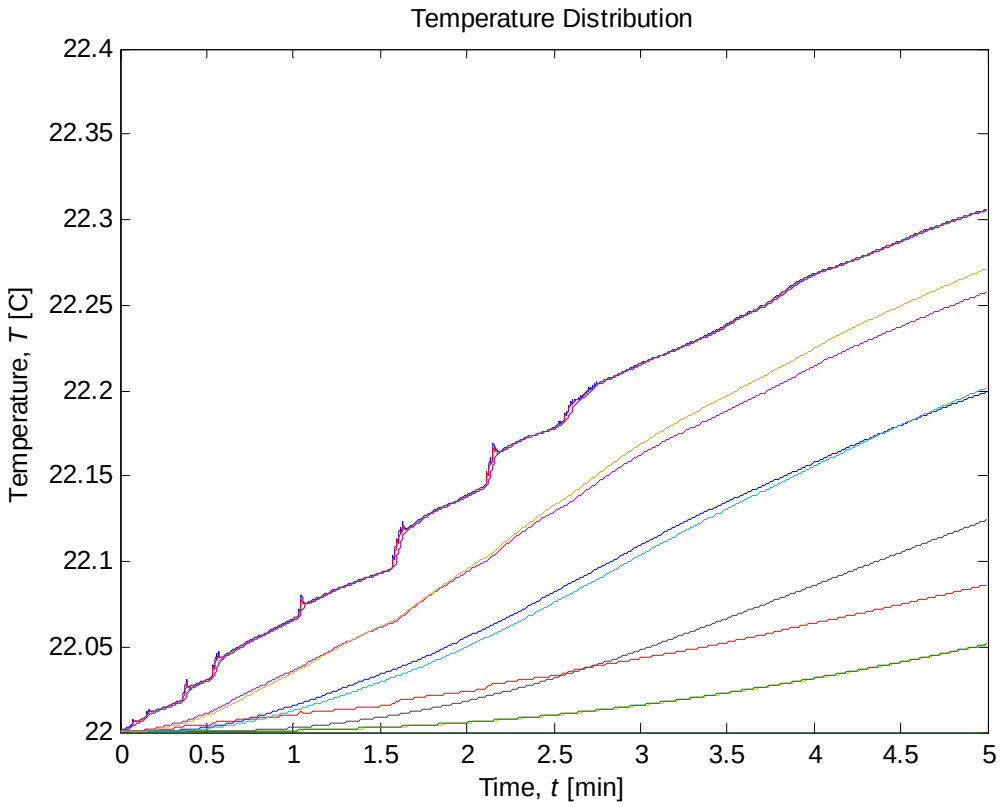

Figure 2.7: Temperature profile of the motor.

Part III – Source Code (foc.m)

```
% Nonlinear Dynamic Modeling and Field Oriented Control
% of Permanent Magnet (PM) Motor
%
% Written in SI or MKS Unit System.
%
% Authors:
%    David Woodburn
%    Dr. Lei Zhou
%    Dr. Thomas X. Wu

clear all; close all; clc;

tic;

% ------------------------
% Input motor parameters.
% ------------------------
motorParameter

% -------------------------
% Load EMA mission profile.
% -------------------------
Mission = xlsread('missionProfile.xlsx'); % Load into mission profile
tN = Mission(:,1).';  % time sequence
xSN = Mission(:,2).'; % stroke sequence
FLN = Mission(:,3).'; % load force sequence
% xSN = xSN * 0.0254; % If stroke is in inch, needs to convert to meter.
% FLN = FLN * 4.4482; % If load force is in lbf, needs to covert to Newton.

theta_meSN = xSN*Ncr*p/2 + theta_meInitial;
tauLN = FLN/(Ncr*effDrive);  % Load torque [N m]

% ------------------------------------------------------
% Set up simulation parameters.
% ------------------------------------------------------
spc = 10;               % Samples per cycle of highest frequency
tauTh = 0.01;           % Thermal time constant [s]

% Set PI coefficients.
kp = 0.1;    % []
ki = 0.0001; % [A s/rad]

% Set differential time-stepping weights.
alpha_dt = 0.5;
beta_dt = 1 - alpha_dt;

% Set motor simulation convergence parameters.
epsilon = 0.0001;   % Convergence limit []
Ncvg = 50;          % Maximum number of convergence iterations

T = tN(end) - tN(1);    % T could have been redefined.
```

```
Nt = length(tN);        % Initial length of profile arrays
nfMax = 1;              % Order of highest frequency harmonic of interest
NtR = round(spc*(nfMax*omega_meLim/(2*pi))*T); % High-res, time steps
dtE0 = T/(NtR-1);                              % Mean hi-res time step
omegaSMin = 2*pi/0.002; % Min sampling frequency [rad sample/s]
omegaSMax = 2*pi/dtE0;  % Max sampling frequency [rad sample/s]

ntR = 2;      % Hi-res index for recording []
NtETotal = 1; % Counter for the total number of simulation points
tTh = 0;      % Last time for thermal calculation [s]

% Pad arrays (for interpolation referencing).  Lengths are Nt+3.
dtBar = mean(diff(tN)); % Note that dt might not be constant.
tN = [tN(1)-dtBar, tN, tN(end)+dtBar, tN(end)+2*dtBar];
theta_meSN = [theta_meSN(1), theta_meSN, theta_meSN(end), theta_meSN(end)];
tauLN = [tauLN(1), tauLN, tauLN(end), tauLN(end)];

% Initialize states.
Rs = Rs_room;       % Initial phase winding resistance [ohm]
id = 0;             % Phase d current [A]
iq = 0;             % Phase q current [A]
did_dt = 0;         % Rate of change of id [A/s]
diq_dt = 0;         % Rate of change of iq [A/s]

Ld0 = LdSN(1);      % Ld at zero current
Lq0 = LqSN(1);      % Lq at zero current
Ld = Ld0;           % Initial Ld
Lq = Lq0;           % Initial Lq

ud = 0;                   % Phase d voltage [V]
uq = 0;                   % Phase q voltage [V]
theta_me = theta_meSN(1); % Start up (Mechanical angle)*p/2 [rad]
omega_me = 0;             % (Mechanical angular frequency)*p/2 [rad/s]
alpha_me = 0;             % (Mechanical angular acceleration)*p/2 [rad/s^2]
Qs = 0;                   % Heat source flux (from windings)
Q = zeros(Nth,1);         % Heat flux
NConverge = 0;            % Counter for number of convergence iterations

% Saturation curve points.
rSat = 0.10;        % Saturation ratio []
i1 = iLim*(1-rSat); % Beginning of current saturation [A]
i3 = iLim*(1+rSat); % Ending of current saturation [A]
u1 = uLim*(1-rSat); % Beginning of voltage saturation [V]
u3 = uLim*(1+rSat); % Ending of voltage saturation [V]
th2L = xMinLim*Ncr*p/2 + theta_meInitial; % theta_me max limit
th2R = xMaxLim*Ncr*p/2 + theta_meInitial; % theta_me min limit
th0 = (th2R + th2L)/2;                    % Midpoint between theta_me limits
th1R = (th2R - th0)*(1-rSat) + th0;
th3R = (th2R - th0)*(1+rSat) + th0;
th1L = -(th0 - th2L)*(1-rSat) + th0;
th3L = -(th0 - th2L)*(1+rSat) + th0;

% Set threshold to show limits in plots.
limThreshold = 0.8; % []
```

```
% ---------------------------
% Initialize recording arrays.
% ---------------------------

% Initialize hi-res arrays.
NtR0 = round(NtR*1.05);    % Add 5% buffer [].
tR = zeros(1,NtR0);        % Hi-res time record [s]
uaR = zeros(1,NtR0);       % Hi-res phase A voltage record [V]
ubR = zeros(1,NtR0);       % Hi-res phase B voltage record [V]
tauLR = zeros(1,NtR0);     % Hi-res load torque record [N m]
theta_meR = zeros(1,NtR0); % Hi-res theta_me record [rad]
omega_meR = zeros(1,NtR0); % Hi-res omega_me record [rad/s]

% Initialize low-res arrays.
tNR = zeros(1,Nt);
theta_meN = zeros(1,Nt);       % Actual theta_me [rad]
theta_meN(1) = theta_meSN(1);
omega_meN = zeros(1,Nt);       % Actual omega_me [rad/s]
idN = zeros(1,Nt);             % Direct current [A]
iqN = zeros(1,Nt);             % Quadrature current [A]
phiN = zeros(1,Nt);            % Torque angle [rad]

LdN = zeros(1,Nt); LdN(1) = Ld0;       % Direct inductance [H]
LqN = zeros(1,Nt); LqN(1) = Lq0;       % Quadrature inductance [H]

udN = zeros(1,Nt);                     % Direct voltage [V]
uqN = zeros(1,Nt);                     % Quadrature voltage [V]
RsN = zeros(1,Nt); RsN(1) = Rs;        % Resistance [ohm]
tauMN = zeros(1,Nt);                   % Machine torque [N m]
PinN = zeros(1,Nt);                    % Power in [W]
PcuN = zeros(1,Nt);                    % Copper loss [W]
PfricN = zeros(1,Nt);                   % Friction loss [W]
TthN = zeros(Nth,Nt); TthN(:,1) = Tth; % Temperature [C]

% ----------------------
% Run through time steps.
% ----------------------

% A low resolution (low-res) profile is analyzed one segment (step) at a
% time, breaking each segment into many sub-segements that have a high
% resolution.  Interpolation is used to accomplish this, and the number
% and size of the time steps are based on an average hi-res time step
% size based on the maximum electrical speed of the motor.  During
% playback, there is only one low-res segment (Nt = 2) and all the
% profile points are hi-resolution.  At that point, the hi-res time step
% size and the number of time steps are based on the pre-recorded hi-res
% time array.  Any technique used for interpolating omega on the low-res
% scale will be yield different results than on the hi-res scale just
% because of the scale, even if the same technique is used.  However,
% using a perfect N-point derivative (PNPD) should yield fairly accurate
% results without averaging.

% For each low-res segment, simulate.
```

```
for nt = 2:Nt
    % Calculate number and size of steps for this segment.
    dt = tN(nt+1) - tN(nt); % Update low-res segment time-step size.

    % Calculate variable, hi-res time step based on dthetaE/dt.
    dtheta_me = theta_meSN(nt+1) - theta_meSN(nt);
    dtheta_meAbs = abs(dtheta_me);
    omegaSAbs = spc*dtheta_meAbs/dt; % spc = samples per cycle
    omegaSAbs = omegaSAbs*(omegaSAbs>omegaSMin) + ...
        omegaSMin*(omegaSAbs<=omegaSMin);
    omegaSAbs = omegaSAbs*(omegaSAbs<omegaSMax) + ...
        omegaSMax*(omegaSAbs>=omegaSMax);
    dtE = 2*pi/omegaSAbs;
    NtE = ceil(dt/dtE) + 1; % Update number of sub, hi-res time points.
    dtE = dt/(NtE-1);       % Update hi-res segments time-step size.

    % Count the total number of simulation points.
    NtETotal = NtETotal + (NtE - 1);

    % Reset micro-loop's energy.
    PcuBar = 0;
    %    This is used to find the average power in a micro loop which is
    %    then used for the thermal component.

    % Simulate this low-res segment in hi-res.
    for ntE = 2:NtE

        % ------------------------------
        % Get inputs to motor simulation.
        % ------------------------------

        % Variables ending in "S" represent desired values.
        % Variables ending in "P" represent next step values.
        % Variables without these are this step's values.

        % The process of getting the inputs to the motor simulation
        % transitions from this time step to the next.  The inputs belong
        % to the resolved (convergent) state of the next time step.
        % Therefore, udP, uqP, tauLP, thetaEP, and omegaEP all belong to
        % the next time step.  The motor simulation accepts certain of
        % those inputs as given values and then resolves the remaining
        % states of the motor such that those inputs could be true.

        % Determine index in Nt scale from index in NtE scale.
        wt = ntE/NtE; % Progress in this nt segment (0 to 1]

        % Use weighting to get t, thetaS, and omegaS.
        t = tN(nt)*(1-wt) + tN(nt+1)*wt;                          % [s]
        tauLP = tauLN(nt)*(1-wt) + tauLN(nt+1)*wt;                % [N m]
        theta_meS = theta_meSN(nt)*(1-wt) + theta_meSN(nt+1)*wt; % [rad]
        dt3 = tN((nt):(nt+2)) - tN((nt-1):(nt+1));                % [s]
        omega_me3 = (theta_meSN(nt:(nt+2)) - ...
            theta_meSN((nt-1):(nt+1)))./dt3;            % [rad/s]
        omega_meS = (wt <= 0.5).*(omega_me3(1).*(0.5 - wt) + ...
```

```
    omega_me3(2).*(0.5 + wt)) + ...
    (wt > 0.5).*(omega_me3(2).*(1.5 - wt) + ...
    omega_me3(3).*(wt - 0.5));      % [rad/s]

% Get theta and omega errors.
eTheta_me = (theta_meS - theta_me); % Mechanical [rad]
eOmega_me = (omega_meS - omega_me); % Mechanical [rad/s]

% Get iqS.
tauM_iq = 3*p/4*(lambdaPM + id*(Ld-Lq)); % [N m/A]
iqS = iq + 2/(p*tauM_iq)*(I*(kp*eOmega_me/dtE - alpha_me) + ...
    c*(kp*eOmega_me)) + ki*eTheta_me/dtE; % [A]

% Set idS.
idS = 0; % id should almost always be zero [A]

% Rate limit iqS (reduces transients).
diqdtS = (iqS-iq)/dtE; % Predicted current rate [A/s]
diqdtS = sign(diqdtS)*min([didtLim,abs(diqdtS)]); % Cap diqdt [A/s]
iqS = iq + diqdtS*dtE; % Rebuilt iqS [A]

% Saturation limit abs of iqS.
iqS = sign(iqS)*((abs(iqS)<i3)*(abs(iqS) - (abs(iqS)>=i1)*...
    ((abs(iqS)-iLim*(1-rSat))^2)/(4*iLim*rSat)) + ...
    (abs(iqS)>=i3)*iLim); % [A]

omega_meP = omega_me + (kp*eOmega_me);

% Calculate inductances based on desired currents.
mLq = (NL-1)*(abs(iqS)-iLMin)/(iLMax-iLMin) + 1;% Unbounded real []
wLq = mod(mLq,1); % Real number [0:1) []
nLq = mLq - wLq;  % Unbounded integer []
LdS = (1-wLq)*LdSN(nLq) + wLq*LdSN(nLq+1); % [H]
LqS = (1-wLq)*LqSN(nLq) + wLq*LqSN(nLq+1); % [H]
% The above is equivalent to using interp1, but much faster.
%             LdS = interp1(iL,LdSN,abs(iqS));
%             LqS = interp1(iL,LqSN,abs(iqS));

% Calculate new voltages.
udS = Rs*idS + LdS*(idS-id)/dtE  - omega_meP*LqS*iqS;  % [V]
uqS = Rs*iqS + LqS*(iqS-iq)/dtE  + omega_meP*LdS*idS + ...
    omega_meP*lambdaPM; % [V]

% Saturation limit abs of voltages.
ud = sign(udS)*((abs(udS)<u3)*(abs(udS) - (abs(udS)>=u1)*...
    ((abs(udS)-uLim*(1-rSat))^2)/(4*uLim*rSat)) + ...
    (abs(udS)>=u3)*uLim); % [V]
uq = sign(uqS)*((abs(uqS)<u3)*(abs(uqS) - (abs(uqS)>=u1)*...
    ((abs(uqS)-uLim*(1-rSat))^2)/(4*uLim*rSat)) + ...
    (abs(uqS)>=u3)*uLim); % [V]

% ----------------------------------------
% Seek convergence for one hi-res time step.
```

```
% ----------------------------------------

% Assume next values from present values.  Simulation should not
% assume any knowledge of "S" values.
idP = id + did_dt*dtE; % [A]
iqP = iq + diq_dt*dtE; % [A]
alpha_meP = alpha_me;  % Angular acceleration [rad/s^2]
omega_meP = omega_me + alpha_me*dtE;

% Run dynamical equations until convergence.
for nConverge = 1:Ncvg

    % Get next inductances by look-up table.
    mLq = (NL-1)*(abs(iqP)-iLMin)/(iLMax-iLMin) + 1;%Unbounded real
    wLq = mod(mLq,1); % Real number [0:1) []
    nLq = mLq - wLq;  % Unbounded integer []
    LdP = (1-wLq)*LdSN(nLq) + wLq*LdSN(nLq+1); % [H]
    LqP = (1-wLq)*LqSN(nLq) + wLq*LqSN(nLq+1); % [H]
    % The above is equivalent to using interp1, but much faster.
    %             LdP = interp1(iL,LdSN,abs(iqP));
    %             LqP = interp1(iL,LqSN,abs(iqP));

    % Get next magnetic and air torques.  p/2 is used to get
    % cummulative torque, not to convert to electrical units.
    tauMP = 3*p/4*iqP*(lambdaPM + idP*(LdP-LqP));        % [N m]
    tauFricP = c*omega_meP*2/p; % [N m]

    % Get next angular acceleration.
    alpha_meP = p/2/I*(tauMP - tauLP - tauFricP);     % [rad/s^2]
    % Comes from tauM = tauL + I*alpha_m, alpha_me = alpha_m*p/2.

    % Get next angular speed and angle.
    omega_meP = omega_me + ...
        (alpha_dt*alpha_me + beta_dt*alpha_meP)*dtE; % [rad/s]
    theta_meP = theta_me + ...
        (alpha_dt*omega_me + beta_dt*omega_meP)*dtE; % [rad]
    % theta_meP is updated here because some parameters might
    % depend on the value of theta_me.

    % Get next currents.  Current should be updated last since it
    % is used for the convergence test.
    didP_dt = 1/LdP*(-Rs*idP + omega_meP*LqP*iqP + ud); % [A/s]
    diqP_dt = 1/LqP*(-Rs*iqP - omega_meP*LdP*idP + uq - ...
        omega_meP*lambdaPM);                % [A/s]
    idP = id + (alpha_dt*did_dt + beta_dt*didP_dt)*dtE;  % [A]
    iqPOld = iqP;
    iqP = iq + (alpha_dt*diq_dt + beta_dt*diqP_dt)*dtE;  % [A]

    % Check for electrical convergence.
    if abs(iqP - iqPOld)/iLim < epsilon % []
        break;
    end
end % end nConverge
```

```
% Add convergence iterations.
NConverge = NConverge + nConverge;

% Update heat generated.
Pcu = 3/2*(iq^2 + id^2)*Rs; % Next-step source heat [W]
PcuBar = PcuBar + Pcu/NtE;

% -----------------
% Simulate thermal.
% -----------------
if t - tTh > tauTh

    % Get next-step winding resistance.
    Rs = Rs_room;

    dtTh = t - tTh;
    tTh = t;

    % Calculate temperatures.
    IC = Pcu/4;  % winding loss (only quarter portion is used)

    % Calculate next-step temperatures.
    TthP(1) = Tth(1) + (IC + (Tth(3)-Tth(1))/Rth(1))/Cth(1)*dtTh;
    TthP(2) = Tth(2);
    TthP(3) = Tth(3) + (IS + (Tth(4)-Tth(3))/Rth(2) + ...
    (Tth(10)-Tth(3))/Rth(12) + (Tth(1)-Tth(3))/Rth(1))/Cth(3)*dtTh;
    TthP(4) = Tth(4) + ((Tth(4)-Tth(14))/Rth(3) + ...
        (Tth(13)-Tth(4))/Rth(14) + (Tth(3)-Tth(4))/Rth(2) + ...
        (Tth(5)-Tth(4))/Rth(4))/Cth(4)*dtTh;
    TthP(5) = (Rth(5)*Tth(4) + Rth(4)*Tth(2))/(Rth(4)+Rth(5));
    TthP(6) = Tth(6) + ((Tth(9)-Tth(6))/Rth(6) + ...
      (Tth(7)-Tth(6))/Rth(7) + (Tth(8)-Tth(6))/Rth(8))/Cth(6)*dtTh;
    TthP(7) = Tth(7) + (-IR7a + (Tth(6)-Tth(7))/Rth(7) + ...
        (Tth(12)-Tth(7))/Rth(9))/Cth(7)*dtTh;
    TthP(8) = Tth(8) + ((Tth(6)-Tth(8))/Rth(8) + ...
        (Tth(13)-Tth(8))/Rth(10))/Cth(8)*dtTh;
    TthP(9) = Tth(9) + (IM + (Tth(6)-Tth(9))/Rth(6) + ...
        (Tth(10)-Tth(9))/Rth(11))/Cth(9)*dtTh;
    TthP(10) = (Tth(3)*Rth(11) + Tth(9)*Rth(12) + ...
        Rth(11)*Rth(12)*IW)/(Rth(11)+Rth(12));
    TthP(12) = Tth(12) + (IBF + (Tth(14)-Tth(12))/Rth(13) + ...
        (Tth(7)-Tth(12))/Rth(9))/Cth(12)*dtTh;
    TthP(13) = Tth(13) + (IBB + (Tth(4)-Tth(13))/Rth(14) + ...
        (Tth(8)-Tth(13))/Rth(10))/Cth(13)*dtTh;
    TthP(14) = Tth(14) + (-IR14 + (Tth(4)-Tth(14))/Rth(3) + ...
        (Tth(12)-Tth(14))/Rth(13))/Cth(14)*dtTh;

    Tth = TthP;
end

% --------------
% Update states.
% --------------
```

```
    id = idP;
    iq = iqP;
    did_dt = didP_dt;
    diq_dt = diqP_dt;
    Ld = LdP;
    Lq = LqP;
    theta_me = theta_meP;
    omega_me = omega_meP;
    alpha_me = alpha_meP;

    % -------------------------
    % Record hi-res variables.
    % -------------------------
    tHR(ntR) = t;
    udH(ntR) = ud;
    uqH(ntR) = uq;
    theta_meR(ntR) = theta_me;
    omega_meR(ntR) = omega_me;
    tauLR(ntR) = tauLP;
    ntR = ntR + 1;

end % end hi-res simulation

% -------------------------
% Record low-res variables.
% -------------------------

% Store time.
tNR(nt) = t;

% Store motor stroke.
theta_meN(nt) = theta_me; % [rad]
omega_meN(nt) = omega_me; % [rad/s]

% Store currents.
idN(nt) = id; % [A]
iqN(nt) = iq; % [A]

% Store inductances.
LdN(nt) = Ld; % [H]
LqN(nt) = Lq; % [H]

% Store voltages.
udN(nt) = ud; % [V]
uqN(nt) = uq; % [V]

% Store resistance.
RsN(nt) = Rs; % [ohm]

% Store motor torque.
tauMN(nt) = tauMP; % [N m]

% Store powers [W].
```

```
    PinN(nt) = 3/2*(iq*uq + id*ud);  % Input power
    PcuN(nt) = 3/2*(iq^2 + id^2)*Rs; % Copper loss for whole motor
    PfricN(nt) = tauFricP*(omega_me*2/p);

    % Store temperatures.
    TthN(:,nt) = Tth;

end % End time stepping.

% Unpad profile arrays.
tN = tN(2:(Nt+1));
theta_meSN = theta_meSN(2:(Nt+1));
tauLN = tauLN(2:(Nt+1));
tR(ntR:end) = [];
theta_meR(ntR:end) = [];
omega_meR(ntR:end) = [];
tauLR(ntR:end) = [];

% ----------------
% Show statistics.
% ----------------

disp('Dynamic Modeling and Field Oriented Control of PM Motor');

% Calculate stroke, speed, and acceleration.
xN = (theta_meN - theta_meInitial)*2/p/Ncr;  % [m]
vN = diff(xN)./diff(tNR);                    % [m/s]
NT = length(tNR);
tNRmid = (tNR(1:NT-1) + tNR(2:NT))/2;        % [s]
aN = diff(vN)./diff(tNRmid);                 % [m/s^2]

% Calculate and Report statistics.
PcuMean = mean(PcuN);        % mean winding power loss [W]
tauMMax = max(abs(tauMN));   % [N m]
tauLMax = max(abs(tauLN));   % [N m]
FMax = tauLMax*Ncr*effDrive; % [N]
vMax = max(abs(vN));         % [m/s]
aMax = max(abs(aN));         % [m/s^2]
dtEMin = min(diff(tHR));     % [s]
dtEMax = max(diff(tHR));     % [s]
spaces = '';
disp([spaces 'Mean winding power loss = ' num2str(PcuMean) ' W ']);
disp([spaces 'Max motor torque = ' num2str(tauMMax) ' N m ']);
disp([spaces 'Max actuator force = ' num2str(FMax) ' N ']);
disp([spaces 'Max velocity = ' num2str(vMax) ' m/s ']);
disp([spaces 'Max acceleration = ' num2str(aMax) ' m/s^2 ']);
disp([spaces 'Min electrical time step = ' num2str(dtEMin) ' s ']);
disp([spaces 'Max electrical time step = ' num2str(dtEMax) ' s ']);

% ------------
% Show graphs.
% ------------

% Stroke
```

```
figure('Name','Stroke');
plot(tN/60, xSN/0.0254, tNR/60, xN/0.0254);
xlswrite('strokeActual.xlsx', [tNR;xN].');
ylabel(['Stroke, \it{x}\rm [in]']);
xlabel('Time, \it{t}\rm [min]');
title('Mechanical Stroke Following');
legend('\it{x_{desired}}','\it{x_{actual}}');

% Torque
figure('Name','Load Force')
plot(tN/60,FLN);
ylabel('Load Force, \it{F_{load}}\rm [N]');
xlabel('Time, \it{t}\rm [min]');
title('Load Force');

figure('Name','Load Torque');
plot(tN/60, tauLN);
ylabel('Load Torque, \it{\tau_L}\rm [N m]');
xlabel('Time, \it{t}\rm [min]');
title('Load Torque');

figure('Name','Magnetic Torque');
plot(tNR/60, tauMN, 'g');
xlswrite('tauM.xlsx', [tNR;tauMN].');
ylabel('Magnetic Torque, \it{\tau_M}\rm [N m]');
xlabel('Time, \it{t}\rm [min]');
title('Magnetic Torque');

% Current
figure('Name','Current');
plot(tNR/60,idN,tNR/60,iqN);
xlswrite('idiq.xlsx', [tNR;idN;iqN].');
ylabel('Currents, \it{i_d}\rm [A] and \it{i_q}\rm [A]');
xlabel('Time, \it{t}\rm [min]');
title('dq Currents');
legend('\it{i_d}','\it{i_q}');

% Voltage
figure('Name','Voltage');
plot(tNR/60,udN, tNR/60,uqN);
xlswrite('uduq.xlsx', [tNR;udN;uqN].');
% xlswrite('uduq.xlsx', [tHR;udH;uqH].'); % for high resolution, very slow
ylabel('Voltages, \it{u_d}\rm [V] and \it{u_q}\rm [V]');
xlabel('Time, \it{t}\rm [min]');
title('dq Voltages');
legend('\it{u_d}','\it{u_q}');

% Copper Loss
figure('Name','Copper Loss');
plot(tNR/60,PcuN/1000);
xlswrite('Pcu.xlsx', [tNR;PcuN].');
ylabel('Power Loss, \it{P_{cu}}\rm [kW]');
xlabel('Time, \it{t}\rm [min]');
title('Power Loss in Windings');
```

```
% Electric Power
figure('Name','Electric Power');
xlswrite('Pin.xlsx', [tNR;PinN].');
PinNN = [];
tNN = [];
n0 = 1;
hold on;
for n = 1:length(tNR)-1
    PinNN = [PinNN, PinN(n)];
    tNN = [tNN, tNR(n)];
    if PinN(n)*PinN(n+1) < 0
        PinNN = [PinNN, 0];
        tadd = tNR(n)+(tNR(n+1)-tNR(n))*abs(PinN(n))/...
            (abs(PinN(n))+abs(PinN(n+1)));
        tNN = [tNN,tadd];
        if PinN(n) > 0
            plot(tNN/60,PinNN,'b');
        else
            plot(tNN/60,PinNN,'r');
        end
        PinNN = 0;
        tNN = tadd;
    end
end
PinNN = [PinNN, PinN(end)];
tNN = [tNN, tNR(end)];
if PinN(end) > 0
    plot(tNN/60,PinNN,'b');
else
    plot(tNN/60,PinNN,'r');
end
ylabel('Power, \it{P}\rm [W]');
xlabel('Time, \it{t}\rm [min]');
title('Electrical Power');
hold off;

% Thermal
figure('Name','Thermal');
plot(tNR/60,TthN([1,2,3,4,5,6,7,8,9,10,12,13,14],:));
xlswrite('temperature.xlsx', [tNR;TthN;].');
ylabel('Temperature, \it{T}\rm [C]');
xlabel('Time, \it{t}\rm [min]');
title('Temperature Distribution');

toc;
```

Part IV – Motor Parameter Code (motorParameter.m)

```
% Define primary motor parameters.(This example is for a Danaher's motor.)
Rs_room = 0.775;               % Phase resistance at room temperature [ohm]
p = 10;                        % Number of poles []
I = 113.2*10^(-6);             % Inertia moment [kg m^2/rad]
c = 0.00001;                   % Friction Coefficient [kg m^2/s rad]
lambdaPM = 0.0793;             % PM flux amplitude [Wb]

% Build direct inductance Ld and quadrature inductance Lq.
% Load current and inductance arrays.
iL = 0:10:300;
LdSN = [4.46928937, 4.435673396, 4.334488681, 4.201478319, ...
    4.055221239, 3.895196891, 3.741845461, 3.59804698, ...
    3.464592095, 3.34851825, 3.250656076, 3.16810712, ...
    3.096573444, 3.033981034, 2.978679457, 2.929048419, ...
    2.884038304, 2.843532188, 2.805950657, 2.77189558, ...
    2.739726553, 2.710652474, 2.683562881, 2.658379174, ...
    2.634980767, 2.612739765, 2.592141217, 2.572607466, ...
    2.553992315, 2.536488402, 2.519800427] * 0.001; % [H]
LqSN = [4.612083555, 4.52697855, 4.276907416, 3.919619295, ...
    3.518989894, 3.09915783, 2.740369271, 2.445203741, ...
    2.199031273, 1.99252454, 1.823051455, 1.684390442, ...
    1.568691069, 1.470728535, 1.386369068, 1.313170018, ...
    1.249202936, 1.192423128, 1.141458078, 1.095896561, ...
    1.054610808, 1.017268661, 0.98309393, 0.951930145, ...
    0.923114329, 0.896516968, 0.871994934, 0.84926359, ...
    0.828084863, 0.808445183, 0.789983231] * 0.001; % [H]

% Define thermal parameters.
Rth = [0.001389; 0.007697; 0.5; 0.001896; 16.0; 0.08577; ...
    9.1358; 16.97; 4.4581; 4.4; 5.933; 37.49; 2.6; 2.6];
% Thermal Resistance [^o C/W]
Cth = [38.85; 0; 82.3; 159.11; 0; 56.03; 14.99; 7.08; ...
    6.72; 0.00176; 0; 13.18; 8.41; 62.56];
% Thermal Capacitance [J / ^o C]
Nth = length(Rth);
Troom = 22;                          % Room Temperature [^o C]
Tth = ones(length(Rth),1)*Troom;
IS = 0;                              % stator loss
IW = 0;                              % winding loss
IBB = 0;                             % rear bearing loss
IBF = 0;                             % front bearing loss
IM = 0;                              % magnet loss
IR7a = 0;
IR14 = 0;

% Get current min and max.
NL = length(iL);
iLMin = min(iL);
iLMax = max(iL);

% Define gear train coupling ratio.
Ncr = 49.8728/0.0254;       % Total Coupling Ratio [rad/m]
```

```
effDrive = 0.76;            % Drive train efficiency []
theta_meInitial = pi/6;% Rotor initial (mechanical angle*p/2)when stroke=0.
kAir = 0.00180297/(2*pi)^1.927/(2*pi*(p*pi)^0.927);

% Define simulation limits.
xMinLim = 0;                % stroke min [m]
xMaxLim = 4.05*0.0254;      % stroke max [m]
tauMLim = 1.9256;           % Motor torque limit [N m]
PLim = 688;                 % Rated output power [W]
uLim = 165;           % Maximum instantaneous voltage allowed per phase [V]
iLim = 19.2;          % Maximum instantaneous current allowed per phase [A]
didtLim = 5*10^4;           % Maximum current change rate allowed [A/s]
vLim = 0.086;               % Maximum speed allowed [m/s]
omega_meLim = vLim*Ncr*p/2; % Maximum mechanical angular speed *p/2 [rad/s]
```